**POLITECNICO DI MILANO**

**III School of Engineering**

**Master Degree in Materials Engineering**


# PREPARATION AND CHARACTERIZATION OF NANOFIBER SCAFFOLD OF POLY(L,L-LACTIDE-CO-ε-CAPROLACTONE) AND POLY(L,L-LACTIDE)

**Supervisor: Prof. Lorenza Draghi**

**Co-supervisor: Prof. Dra. Wang Shu Hui and**

**Eng. Helena Oyamana**

**Isabela Najla Saddi ROSA**

**Matr. 734838**

**Academic year: 2010/2011**

# CONTENTS

## LIST OF FIGURES

## LIST OF TABLES

## ABSTRACT

Electrospinning is a non-woven scaffold production process involving the application of a high voltage between a metal syringe needle connected to an injection pump containing the polymer solution and a collector. The increasing of the electric field causes charge induction within the polymer solution, resulting in charge repulsion and the formation of electrostatic forces. These forces oppose to the surface tension of the solution and when a critical voltage is reached, the charge repulsion overcomes the surface tension, causing the initiation of a jet. While the polymer jet travels in a random motion toward the collector the solvent evaporates. In this work, the copolymer poly(L,L-lactide-co-ε-caprolactone) (PLCL) was blended in solution with poly(L,L-lactide) (PLLA) and process parameters, such as applied voltage, flow rate and concentration, were varied until obtaining a fibrous defect-free scaffold. Its morphology was characterized by thermal analysis (DSC) and scanning electron microscopy (SEM); mechanical properties were evaluated by tensile testing and tear resistance. Finally, these PLLA:PLCL substrates were seeded with porcine aortic valve cells and maintained under static culture conditions up to 7 days. At different times of culture, membranes were fixed and visualized by confocal laser scanning microscopy (CLSM) and SEM to evaluate membrane biocompatibility, observed as cell adhesion and colonization within it. Cellular growth was evaluated by MTT assay. The presence of viable cells confirmed its biocompatibility under these conditions. These results demonstrate the feasibility of this method in the production of scaffolds useful for tissue engineering applications.

## SOMMARIO

L’*Electrospinning* è un processo di preparazione di *scaffold* non tessuti che consente la preparazione di nano fibre applicando un campoo elettrico molto intenso tra l´ago di una siringa (collegata ad una pompa di iniezione, contenente la soluzione del polimero da elettrofilare) e un colletore metallico. L'aumento del campo elettrico provoca l'induzione di carica all'interno della soluzione di polimero, con conseguente repulsione di carica e formazione di forze elettrostatiche che si oppongono alla tensione superficiale della soluzione. Quando una tensione critica viene raggiunta, la repulsione di carica supera la tensione superficiale, provocando la formazione di un getto continuo. La velocità del getto e l’evaporazione del solvente portano alla deposizione sul collettore di strutture porose costituite da fibre con diametri inferiore al micrometro.

In questo lavoro, sono stati utilizzati il copolimero poli(L,L-lattide-co-ε-caprolattone) (PLCL) miscelato nella soluzione da elettrofilare con poli(L,L-lactide) (PLLA) e i parametri di processo, come la tensione applicata, portata e concentrazione, sono state variate fino ad ottenere un *scaffold* provi di difetti (Immagine 1). La morfologia dei prodotti ottenuti è stata caratterizzata tramite analisi termica (DSC) e microscopia elettronica a scansione (SEM), mentre le proprietà meccaniche sono state valutate da prove di trazione e resistenza allo strappo.

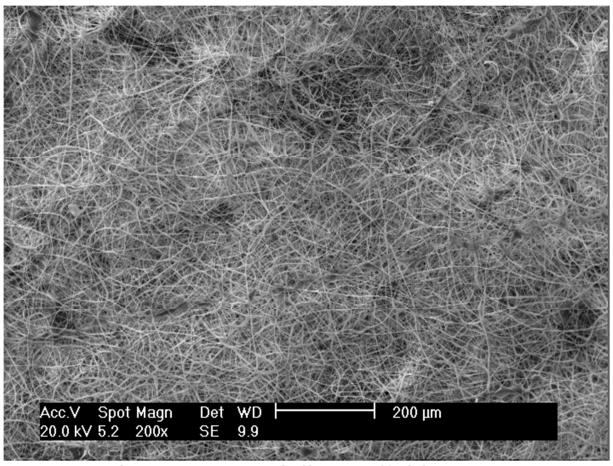


*Immagine 1 – SEM dello scaffold PLLA:PLCL.*

Infine, i substrati du PLLA:PLCL sono stati seminati con cellule prelevate da valvola aortica suina e mantenuti in condizioni di coltura statica fino a 7 giorni. Ad intervalli prestabiliti, le membrane sono stati fissate e osservate mediante microscopia confocale a scansione laser (CLSM) e SEM (Immagine 2) per valutare l' adesione e la colonizzazione cellulare. La vitalità cellulare è stata invece valutata tramite test MTT.

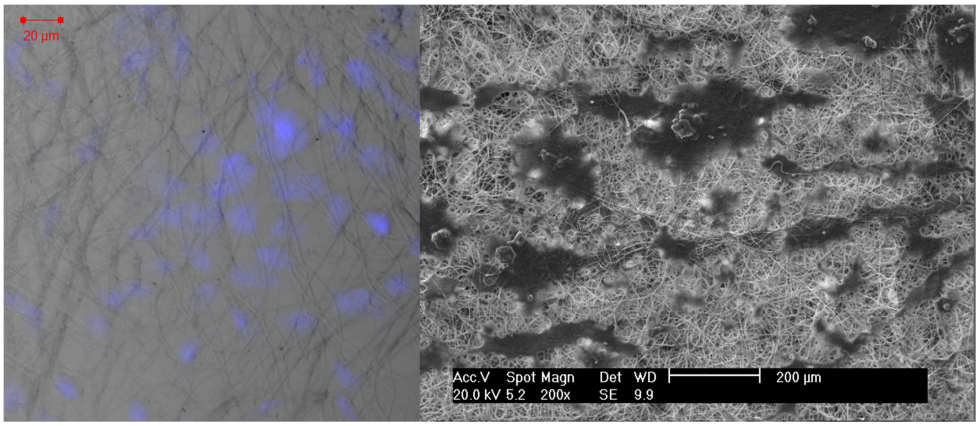


*Immagine 2 – Scaffold dopo la semmina: CLSM dopo 7 giorni di coltura a sinistra e SEM dopo 4 giorni a destra dello.*

La presenza di cellule vitali ha permesso di confermare la biocompatibilità dei substrati preparati nell'arco del lavoro. Nel complesso i risultati ottenuti dimostrano la adeguatezza sia del materiale che della tecnica di preparazione dei supporti per la preparazione di *scaffold* utilizzabili per applicazioni in ingegneria dei tessuti.

# 1. INTRODUCTION

## *1.1. Biomaterials and Biocompatibility*

"Biocompatibility refers to the ability of a biomaterial to perform its desired function with respect to a medical therapy, without eliciting any undesirable local or systemic effects in the recipient or beneficiary of that therapy, but generating the most appropriate beneficial cellular or tissue response in that specific situation, and optimizing the clinically relevant performance of that therapy" [1].

According to Williams [1] definition of biocompatibility, it is possible to understand that a biomaterial should not produce any significant adverse effect to its host, but instead should allow passively or actively a beneficial effect. Therefore, a biomaterial must have the ability to exist in contact with natural tissues without causing any undesirable response to the body. On the contrary, it should perform assessment, monitor, treatment, enhancement, replacement or should facilitate the regeneration of tissues, organs or function.

Since any extraneous material in contact with natural tissue will cause different effects according to the environment [1], biomaterials should be designed for a specific application. Different variables can influence the material and host interaction (*Table 1*) and many effects are possible (e.g. protein adsorption and desorption, cytotoxic effects, fibrosis, micro vascular changes, clotting cascade, antibody production, mutagenic responses and tumor formation) and these interactions could be responsible for the failure or success of the implant [1].

***Table 1 –*** *Variables that can influence the host response to a material* **[1]**.

| |
|---|
| Bulk material composition, micro- (or nano)-structure, morphology |
| Crystallinity and crystallography |
| Elastic constants |
| Water content, hydrophobic–hydrophilic balance |
| Macro-, micro-, nano-porosity |
| Surface chemical composition, chemical gradients, surface molecular mobility |
| Surface topography |
| Surface energy |
| Surface electrical/electronic properties |
| Corrosion parameters, ion release profile, metal ion toxicity (for metallic materials) |
| Degradation profile, degradation product form and toxicity (for polymeric materials) |
| Leachables, additives, catalysts, contaminants and their toxicity (for polymeric materials) |
| Dissolution/degradation profile, degradation product toxicity (for ceramic materials) |
| Wear debris release profile |

Biomaterials are present in many applications that include tissue engineering, invasive sensors, drug delivery and gene transfection systems, nanotechnologies and biotechnology in general and medical devices (*Table 2*) [1].

***Table 2 –*** *Examples of biomaterials and their applications in long term devices* **[1]**.

| Material | Applications |
|---|---|
| Titanium alloys | Dental implants, femoral stems, pacemaker cans, heart valves, fracture plates, spinal cages |
| Cobalt–chromium alloys | Bearing surfaces, heart valves, stents, pacemaker leads |
| Platinum group alloys | Electrodes |
| Nitinol | Shape memory applications |
| Stainless steel | Stents, orthopaedic implants |
| Alumina | Bearing surfaces |
| Calcium phosphates | Bioactive surfaces, bone substitutes |
| Carbon | Heart valves |
| UHMW polyethylene | Bearing surfaces |
| PEEK | Spinal cages |
| PMMA | Bone cement, intraocular lenses |
| Silicones | Soft tissue augmentation, insulating leads, ophthalmological devices |
| Polyurethane | Pacemaker lead insulation |
| Expanded PTFE | Vascular grafts, heart valves |
| Polyester textile | Vascular grafts, heart valves |
| SIBS[a] | Drug eluting stent coating |

Therefore selecting a material as well as designing its final structure for the desired application is an important issue. More specifically, when choosing a biomaterial for a medical application, the requirements to be satisfied are (i)

biocompatibility; (ii) sterilizability[1]; (iii) adequate physical and mechanical properties and (iv) manufacturability, i.e. be easily processed into its final form [2,3]. Moreover, for biodegradable devices it is necessary that the mechanical properties and degradation rate are compatible with the application needs, i.e. the material should have enough resistance and integrity to keep its purpose until the end of its function [3].

According to its application, the proper polymeric biomaterial can be chosen among those presenting biostable (non-degradable), bioresorbable (biodegradable) or partially biodegradable nature [2]. Bioresorbable polymers maintain their supporting properties for a certain period of time and are gradually degraded into harmless substances which are absorbed or eliminated by the organism while being replaced by new tissues [2]. Examples of applications are resorbable sutures, bone fixation devices, tendon or ligament fixation tacks and urological and cardiovascular stents [2]. An advantage of using biodegradable devices is the elimination of a second surgical event for its removal [2,3]. In addition, using this type of polymer decreases the risk of complications associated with the long-term presence of a foreign body in contact with the tissues [4].

Among resorbable materials, it is possible to distinguish natural or synthetic polymers. The natural derived materials have the advantage of higher biological recognition when confronted to synthetic ones. However, a part from being limited in supply and significantly more expensive, they may exhibit immunogenicity and pathogenic impurities, their mechanical properties, biodegradability, and reproducibility are less controllable [5,6] and sterilization is more difficult.

[1] The sterilizability should also be considered for a biomaterial since impurities and contaminations can cause a different response of the human body [8] and, more specifically to nanofibers, some traditional manners to sterilize a material such as heat or γ–irradiation cannot be used since the fibers could be damaged. Nanofibrous scaffolds can be effectively sterilized by ultraviolet light (UV) and ethanol [7].

On the contrary, synthetic polymers are reproducible in large scale production with well controlled properties [5, 6]. Additionally, these materials can be modified to achieve the desired properties associated to a specific implant application [6, 7].

One way to accomplish biodegradation is to synthesize polymers that have hydrolytically unstable linkages in their backbone, which include the most common functional groups such as esters, anhydrides, orthoesters and amides [3].

Among polyesters, polyglicolide (PGA) and polylactide (PLA) are often preferred. Both polymers are prepared by ring opening polymerization and suffer bulk degradation [8].

Lactide is the cyclic dimer of lactic acid, which exists in two optical isomers – dextrorotatory (D) and levorotatory (L) – due to the presence of a chiral carbon. The naturally occurring one is the levorotatory (L) that can originate poly(L,L-lactide) (PLLA) (*Figure 1* ). This polymer presents around 37% crystallinity, high tensile strength and low elongation [3]; PLLA has a melting point ($T_m$) around 170$^oC$ and a glass transition temperature ($T_g$) around 60 $^oC$ [8].

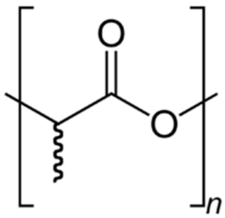


***Figure 1 –*** *Structural formula of PLLA.*

Polymers derived from lactide are biodegradable, and generate lactic acid during its hydrolysis [8]. Furthermore, the acid is eventually eliminated in the form of carbon dioxide and water [5], which is essential for its good performance, considering that even though the lactic acid is present in the body when in high concentration it can reduce the local pH and cause an inflammatory response [4, 8].

As a result, these polymers have been getting attention due to their biocompatibility, non-toxicity and non-immunogenic properties [9]. A few applications of these polymers are sutures, orthopedic fixation, drug delivery systems and scaffolds in tissue engineering [3, 8].

Frequennlty encountered as a biomaterial is also poly(ε-caprolactone) (PCL) (*Figure 2*), a semi crystalline polymer, with a melting point of 59-64$^{o}$C and glass transition temperature of -60$^{o}$C that is also synthesized by ring opening polymerization [3, 8].

Among various types of biomaterials, poly(ε-caprolactone) (PCL) has many advantages because of its biocompatibility, low cost, easy processability and slow hydrolytic degradation rate. PCL has a hydrophobic surface and lacks functional groups. Thus, it is not a good substrate for cell adhesion [10]. The PCL biodegradation is slower than that of PLLA and so it is useful in drug delivery system [8].

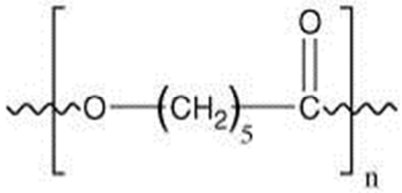


***Figure 2 –*** *Structural formula of PCL.*

PCL and PLLA are normally synthesized by bulk, solution or suspension polymerization and the mechanism of the reaction is coordination [4]. In any case, an organometallic initiator is used in the presence or not of a co-initiator with active hydrogen. The most common initiator is stannous octanoate ($SnOct_2$), which additionally controls the microstructure of the formed polymer [11].

In *Table 3* properties of both polymers, PLLA and PCL, are displayed. They are semi crystalline and so have slow degradation rate. In fact, PLLA and PCL can

take many years to be absorbed by the body. However, the degradation rate does not depend only on the polymer crystallinity but also on its molecular mass, porosity, size and shape of the implant [4].

***Table 3*** *– Summary of a few properties of PLLA and PCL* **[3]**.

| | $T_m$ ($^oC$) | $T_g$ ($^oC$) | Modulus (GPa) | Elongation (%) | Degradation time (months) |
|---|---|---|---|---|---|
| PLLA | 173-178 | 60-65 | 2.7 | 5-10 | >24 |
| PCL | 58-63 | -65- -60 | 0.4 | 300-500 | >24 |

As observed before, one of the advantages of using synthetic polymers is the possibility of balancing properties, and consequently adjust the final performance of the implant for a desired application. For example, PLLA suffers faster degradation than PCL but has lower permeability or PLLA is fragile and PCL is ductile [11]; one strategy to design a material with some intermediate properties is the copolymerization.

The final property of a copolymer is related not only to the relative concentration and properties of the monomers, but also to the microstructure. Therefore, judicious copolymerization reactions of a large variety of existing monomers, can lead to many copolymers and properties [11]. Poly(L,L-lactide-co-ε-caprolactone) (PLCL) (*Figure 3*) is an interesting candidate as biomaterial.

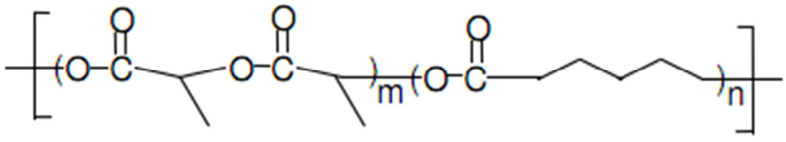


***Figure 3 –*** *Structural formula of PLCL* **[11]**.

There are currently six Food and Drug Administration (FDA)[2] approved poly(α-hydroxyl esters), including poly(glycolide) (PGA), poly(L,L-lactide) (PLLA), poly(D,L-lactide) (PDLLA), poly(D,L-lactide-co-glycolide) (PLGA) (50:50) and (85:15) and poly(ε-caprolactone) (PCL), that have been successfully used to produce nanofibers. However, only PLLA and PCL have slow degradation rates suitable for cell culture applications [7]. This result supported by their biocompatibility and biodegradability demonstrate their potential in tissue engineering [12].

## *1.2. Tissue engineering and scaffolds*

"Tissue Engineering is the creation of new tissue for the therapeutic reconstruction of the human body, by the deliberate and controlled stimulation of selected target cells through systematic combination of molecular and mechanical signals" [1].

In order to achieve this goal, one possible strategy is to perform cell growth in a 3D structure (scaffold) that supports and organizes its growth to reach an adequate architecture [13].

This approach requires designing a polymeric structure with mechanical and biological properties similar to the native extracellular matrix (ECM) in order to best modulate cellular behavior (migration, proliferation and differentiation) [14]. Because in a native tissue environment cells are in contact with the ECM, which acts both as a structural supporter and a regulator of the cell activities [7]; and fiber morphology ranges from nanometer to micrometer scale [12]. Since ECM influences aspects of the cell behavior, it is necessary to recreate the most similar natural environment

[2] Food and Drug administration (FDA) is a division from US Department of Health and Human Services responsible for protecting, regulating and assuring that food, drug, cosmetics, vaccines, other biological products and medical devices are safe and effective for human use (http://www.fda.gov/).

(chemical composition, morphology, surface functional groups), when designing a scaffold for tissue engineering [12]. Furthermore, the mechanical and tensile properties of the membrane also influence the cell behavior and should also be considered [15].

Therefore, scaffold is a 3D substrate that acts as a temporary ECM for cells until the repair or regeneration of the living tissue [5]. Although the desired characteristics of a scaffold are dependent on the specific application, there are a few properties that are generally desirable.

The substrate should be biocompatible, bioresorbable and porous with a high surface area to allow cellular attachment and penetration, cell–cell and cell–matrix communication as well as exchange of nutrients and products of degradation [4, 5, 12]. It should mimic native ECM both functionally and architecturally [12, 14], as it is known that topography of the material affects cellular behavior [9, 15].

Chen [10] indicated that the topology of the surface of the material did affect the adhesion and proliferation of the cells comparing the cell behavior in a PCL plain substrate and a nanofibrous scaffold produced by electrospinning process. According to the work, the cells were not attached to the plain substrate due to the lack of binding sites for the cells to adhere, which was largely improved by higher surface area scaffolds as those produced by electrospinning. Moreover, Chen [16] also showed that cells tend to attach and proliferate more in scaffolds with smaller fiber diameter, also due to higher surface area of the substrate.

Additionally, the scaffold degradation rate must match the rate of growth of the new tissue, in order to maintain its structural integrity through the whole period of time that the implant is needed [4, 5, 6, 12]. Furthermore, the scaffold should have suitable surface chemistry for cell adhesion, proliferation and differentiation [4, 5].

“The biocompatibility of a scaffold or matrix for a tissue engineering product refers to the ability to perform as a substrate that will support the appropriate cellular activity, including the facilitation of molecular and mechanical signaling systems, in order to optimize tissue regeneration, without eliciting any undesirable local or systemic responses in the eventual host” [1].

It is important to observe that there is a difference between the requirements for a biodegradable material for a medical device and a biodegradable scaffold material. The first should not interfere with any biological process, and the second should support it. Therefore, the scaffolds functions are to determine the shape of the new tissue and facilitate the appropriate cellular behavior, which is influenced also by the hydrophilicity and porosity, including pore size and distribution [1].

Among all the candidate materials, polymers are recognized superior due to its biodegradability and processability as well as easier control of its microstructure and mechanical properties [4].

Scaffolds can be produced by many different techniques, some of them are summarized in *Table 4*, and are very briefly described in the following together with examples of basic preparation procedures.

It is necessary to observe that in most techniques a toxic solvent is used, it should be completely removed from the final structure, since its presence can jeopardize the growth and proliferation of the cells [8].

***Table 4 –*** *Some techniques to produce a porous scaffold (adapted from* **[8]***).*

| | Pore dimension (μm) | Porosity (%) | Properties |
|---|---|---|---|
| Fiber bounding | 20-100 | <95 | Low mechanical properties |
| Solvent casting or particulate leaching | 30-500 | 20-80 | Non uniform pores<br>Presence of traces of porogen particles |
| Gas foaming | 50-600 | 20-90 | Interconnected pores but non uniform |
| Freeze-drying or emulsion | <200 | <97 | Interconnected pores |
| 3D printing | 45-150 | <60 | 100% interconnected pores |
| Fused deposition modeling | >150 | <80 | 100% interconnected pores |

Solvent casting-particulate leaching consists on preparing a polymer solution with or without porogen particles. When porogen agent is present, after the evaporation of the solvent, a second solvent is added that dissolves only those particles. Therefore, the prepared scaffold presents a porous structure according to the size, form and quantity of the porogen particles (*Figure 4*) [5, 8, 17]. Among the advantages, we can mention the simple operation, adequate control of pore size and porosity by the size of the particles and its relative concentration in the polymer matrix [5]. On the other hand, there are disadvantages, such as the difficulty to remove soluble particles within the polymer matrix, thus the method is not adequate to produce thick substrates [5]. In addition, the final structure often does not have sufficiently interconnected pores, which limits the uniform cell seeding and tissue growth [5].

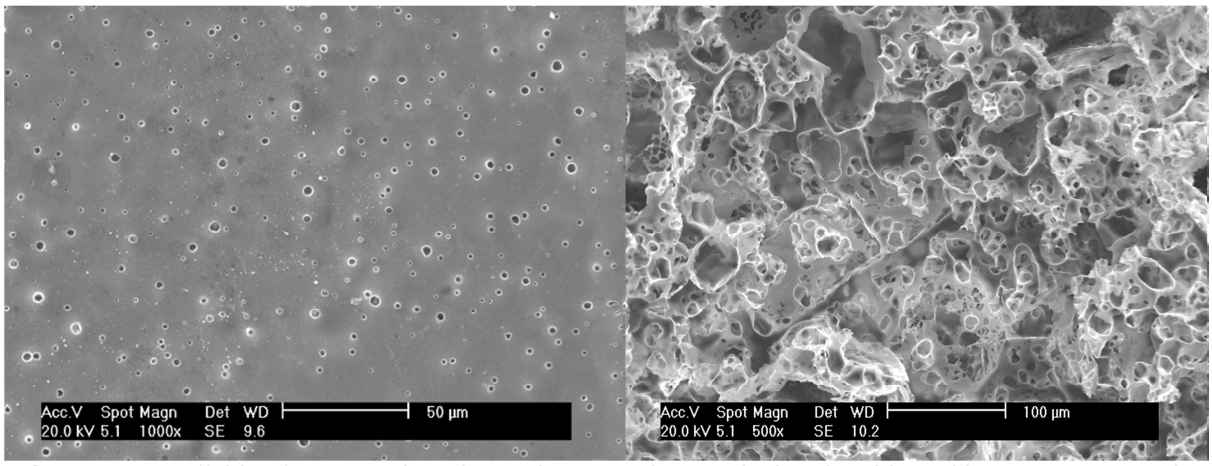


***Figure 4 –*** *Scaffolds of PCL produced as solvent casting-particulate leaching without porogen on the left and with porogen particles to the right.*

Another technique employed for the preparation of a porous scaffold is gas foaming, in which the organic solvent is replaced by a liquefied gas that acts also as porogen agent. Basically, a polymer is saturated with a gas (usually $CO_2$) under high pressure, followed by decreasing until the atmospheric pressure, causing desorption of the gas and the formation of pores within the structure [5, 8, 17]. The major disadvantage of this method is the formation of a closed-pore structure [5].

The freeze-drying technique consists of creating an emulsion from a polymer solution (in an organic solvent) and water, rapidly cooling the emulsion and removing the solvent and water [5]. The dimension of pores is indirectly proportional to the velocity of freezing, i.e. the faster the cooling the smaller the pores formed (*Figure 5*) [8].

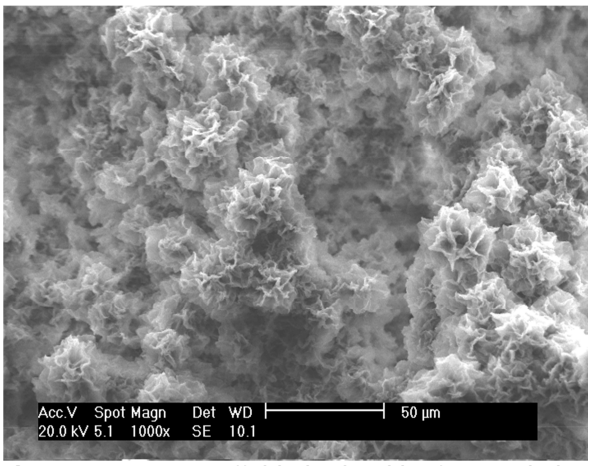


***Figure 5 –*** *PCL scaffold obtained by freeze-drying.*

In thermally induced phase separation the polymer is first dissolved in a solvent at a high temperature, and then the temperature is slowly decreased. With the removal of the solidified solvent-rich phase by sublimation, a porous polymer scaffold is formed. The porous morphology of the scaffolds is dependent on the polymer, solvent, concentration and temperature. One advantage of this method is the good mechanical properties of the final structure [5].

There are many other techniques to produce a porous scaffold, including some non-traditional such as 3D-printing and fused deposition modeling that allows the preparation of more reproducible scaffolds.

## *1.3. Electrospinning*

### 1.3.1. Method and parameters

A simple and inexpensive method to produce a polymer scaffolds is the electrospinning process, which basically uses an electric field to produce fibers from less than 3nm to over 1μm [18, 19], which are deposited on the top of a collector. The apparatus consists basically of a high voltage source, a syringe pump with metal needle to control the flow rate and a conductive collector (*Figure 6*).

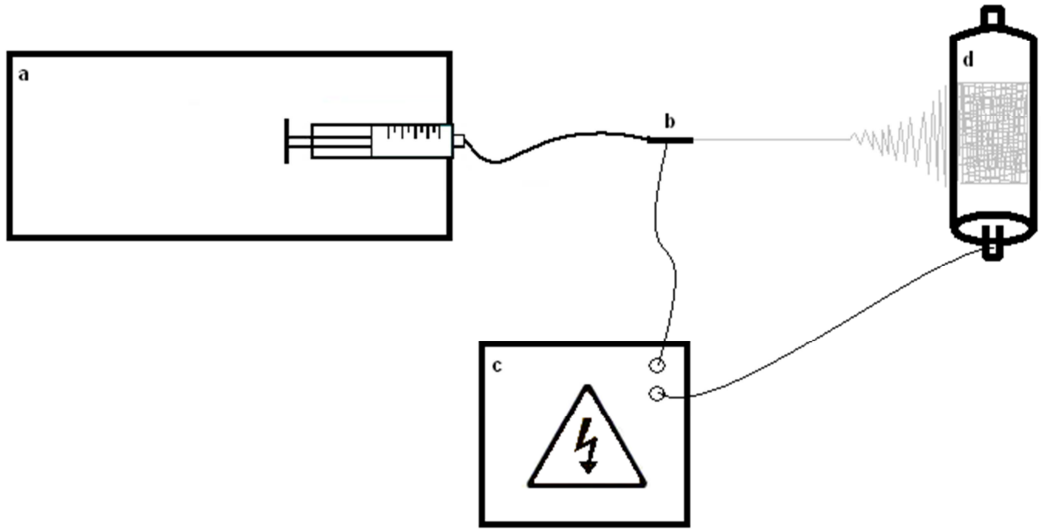


***Figure 6 –*** *Scheme of the electrospinning apparatus a) pump injector, b) metal needle, c) high voltage source and d) metal collector.*

The process involves the application of a high voltage between the tip of a metal syringe needle, where a drop of polymer solution is held by surface tension and the collector. The increasing of the electrical field causes charge induction within the polymer solution, resulting in charge's repulsion and the formation of electrostatic forces. These forces oppose to the surface tension and further increments cause a change in the droplet shape – the hemispherical droplet becomes conical, which is referred to as Taylor cone [20]. When a critical voltage is reached, the charge repulsion overcomes the surface tension, causing the initiation of the jet. While the polymer jet travels in random motion toward the metal collector (that is also the opposite electrode) the solvent evaporates, and the result is a non-woven fiber scaffold [7, 14, 21, 22].

A stable electrospinning jet has four distinct regions that are (i) the base region, where the jet emerges; (ii) the jet region, area the jet travels through; (iii) splaying region, where the jet gets divided and (iv) the collection region [23]. On the region (i) the jet is conical and the velocity of the liquid increases as the polymer is accelerated along the axis of the jet. In the jet region (ii) the electrical forces, which

are resisted by the elongational viscosity of the jet, continue to accelerate the polymer liquid and to stretch the jet, decreasing its diameter. The third region occurs when the electrical charges become larger than the cohesive forces within the jet, and the single jet divides into many charged ones [23].

More recently, confronting this initial idea, Shin [24] has used a high-speed photography to demonstrate that the jet that appears to splay is actually a single unstable one that begins to whip with high frequency and undergoes bending and stretching.

In any case, in the region (iii), in opposition to the region (ii) where the jet is kept straight by the longitudinal stress caused from the electrostatic forces, the jet perpetuate in chaotic motion [18].

Because the polymer solution is charged during the electrospinning process, it is necessary to dissipate those charges, as this will affect how fibers repel each other and how the fibers will arrange themselves on top of the collector. Furthermore, the nature of the targets can affect the diffusion and evaporation of the residual solvent and may also influence the fiber structure. Therefore, the collector's conductivity affects the final fiber packing [25].

Liu [25] confirmed this fact by studying collectors with different conductivities such as copper mesh, aluminum foil and paper. A better conductive collector dissipates more easily the electric charges and so reduces the repulsion among fibers, thus favoring a highly packed membrane. In contrast, when using a less conductive collector a less packed scaffold will be formed, because of the presence of residual electrostatic charges.

Wannatong [26] instead studied the effects of the solvents on the electrospinning process and obtained as result a strong correlation between the solvent properties and the morphology of fibers. In order to prove this correlation, the

author studied the electrospinning of polystyrene (PS) in different solvents like acetic acid, acetonitrile, m-cresol, toluene, N,N-dimethylformamide (DMF) and tetrahydrofuran (THF). Briefly, the density and the boiling point of solvents were found to affect the quantity of residual solvent in the collector; the solubility may lead to the formation of defects; and the fiber diameters were found to decrease exponentially with an increase in the boiling point of the solvents [26].

Varying the solvent is also possible to decrease the surface tension that is the opposite force to the electrical forces responsible for electrospinning. Fong [27] used this fact and studied the effect of substituting water by ethanol on the electrospinning of PEO – the higher the quantity of ethanol, the lower the surface tension of the solution. The result was smoother fibers with larger diameters when more ethanol was used in the process (*Figure 7*).

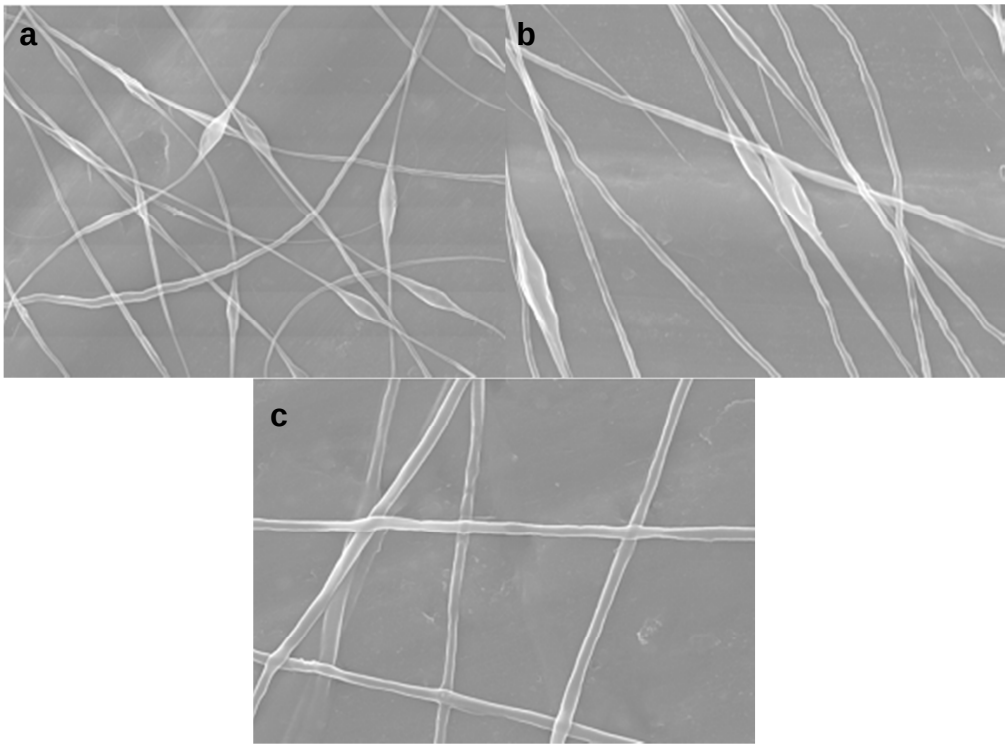


***Figure 7 –*** *Effect of lowering the surface tension for electrospinning of PEO 3% in ethanol and water in ratio equal to (a) 0.054, (b) 0.260 and (c) 0.702* **[27]***.*

In general, volatile solvents are used in the electrospinning to facilitate its removal during the process, but an excessive volatility may cause jet instability or clogging at the needle tip [28]. For materials in biomedical applications, chloroform is a more appropriate solvent for electrospinning, as its low boiling point decreases the chance of solvent remaining in the scaffold [29].

The parameters that control the electrospinning process are (i) solution properties, including viscosity, conductivity, surface tension, polymer molecular mass, dipole moments, and dielectric constant; while the (ii) process variables include, distance between needle and collector, applied voltage and flow rate; in addition to the (iii) ambient parameters, such as temperature, humidity and air flow [30].

Electrospinning will occur when the electrical forces overcome the surface tension[3], and so the formation of defects is the response of the surface tension of the solution trying to decrease the surface area by changing the jet into spherical droplets. On the contrary, the electrical forces tend to elongate the jet, i.e. decrease its diameter [27, 28].

Therefore, lowering this property less defects will be presented in the final scaffold [30]. However, not necessarily solvents with lower surface tension will be chosen for electrospinning [19], as other parameters influence the process.

The viscosity of the polymer solution is directly correlated to the polymer concentration and it is the most critical parameter influencing the nanofiber uniformity, morphology and size [14, 27]. In fact, a higher concentration will result in the formation of fewer defects (beads and diameter enlargement) and consequently a more uniform scaffold [27, 31, 32] (*Figure 8*).

[3] The surface tension other than dependent of the solvent will be affected by the needle diameter, because smaller diameters have smaller ratios at the tip, thus increasing the surface tension and slowing down the jet that will have a longer flight time, and, therefore, more time to be elongated, resulting in smaller fiber diameter [28].

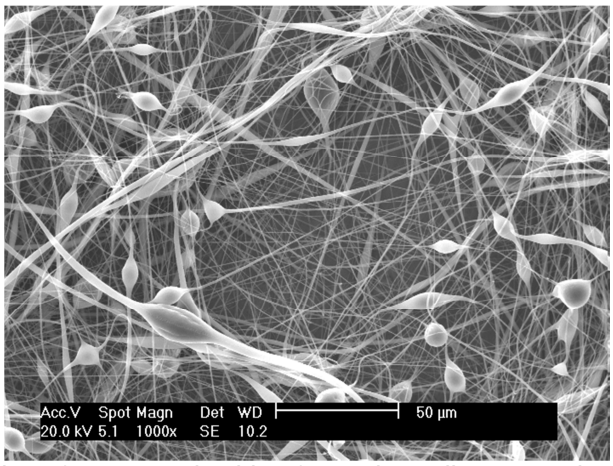


***Figure 8 –*** *Electrospinning of 20% PCL in chloroform where diameter enlargements can be noticed.*

The reason for this effect is the need of chain entanglements (chain overlap) to the fiber formation in electrospinning that will prevent the jet to break into droplets. However, this does not mean that only high molecular mass polymers can be used for electrospinning, instead the presence of enough intermolecular interaction is sufficient for the process to occur.

The influence of this parameter in the fiber diameter is verified by different authors [19, 22, 32-34]; the higher the concentration of the polymer solution, larger are the fibers formed (*Figure 9*).

This fact leads to the thought that smaller fibers diameter could be achieved by decreasing polymer concentration. However it was found to have a limitation in order to obtain uniform defect free scaffolds [12].

This occurs, according to Deitzel [22], because at low viscosities surface tension is the dominant influence on fiber morphology and drops will be form instead of fibers. At high concentrations, processing will be difficult due to the cohesive nature of the high viscosity solution. Moreover, for highly concentrated solutions the droplet may dry out at the tip before the jet is initiated [31].

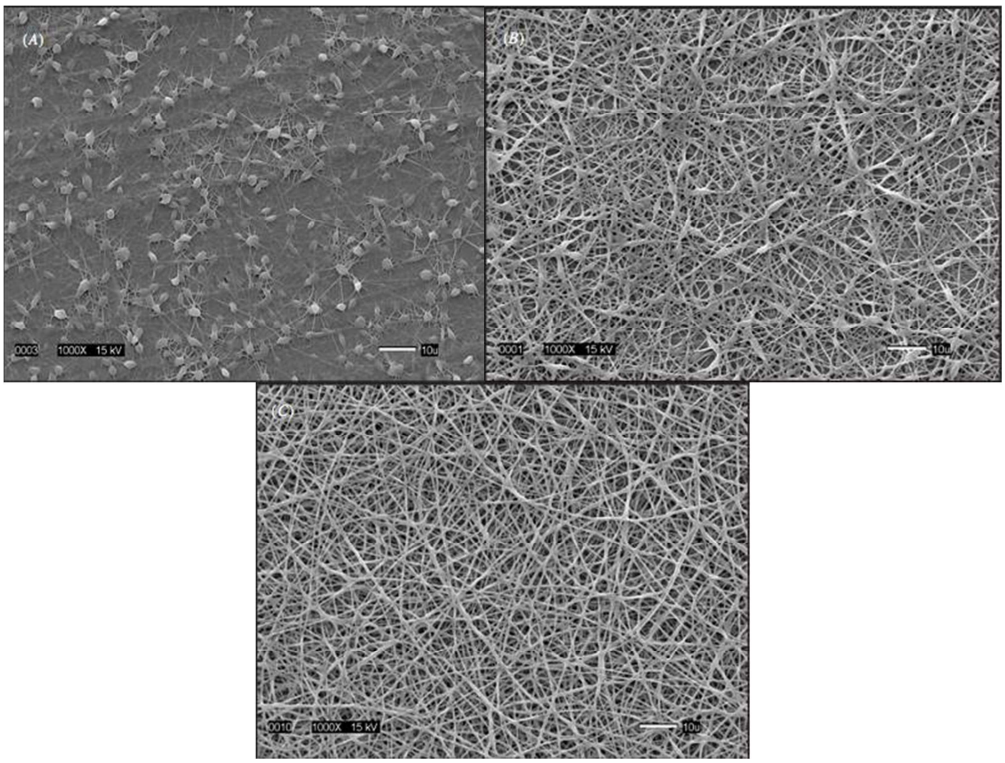


***Figure 9 –*** *Example of solution concentration (a) 4%, (b) 12% and (c) 15% on electrospinning of PLCL. At lower concentrations more defects are present and the fiber diameter increased with the increase of concentration* **[32]**.

A third solution parameter that affects the formation of defects is the polymer solution conductivity, which is determined by the nature of the polymer and solvent, and the presence of ions. It has been shown that a more conductive polymer solution that carries more electric charges tends to produce more uniform fibers [7, 31]. One approach to increase the solution conductivity is through the addition of ionizable salts (*Figure 10*) [31].

The process parameters that are controllable during electrospinning are applied voltage, distance between collector and needle and flow rate.

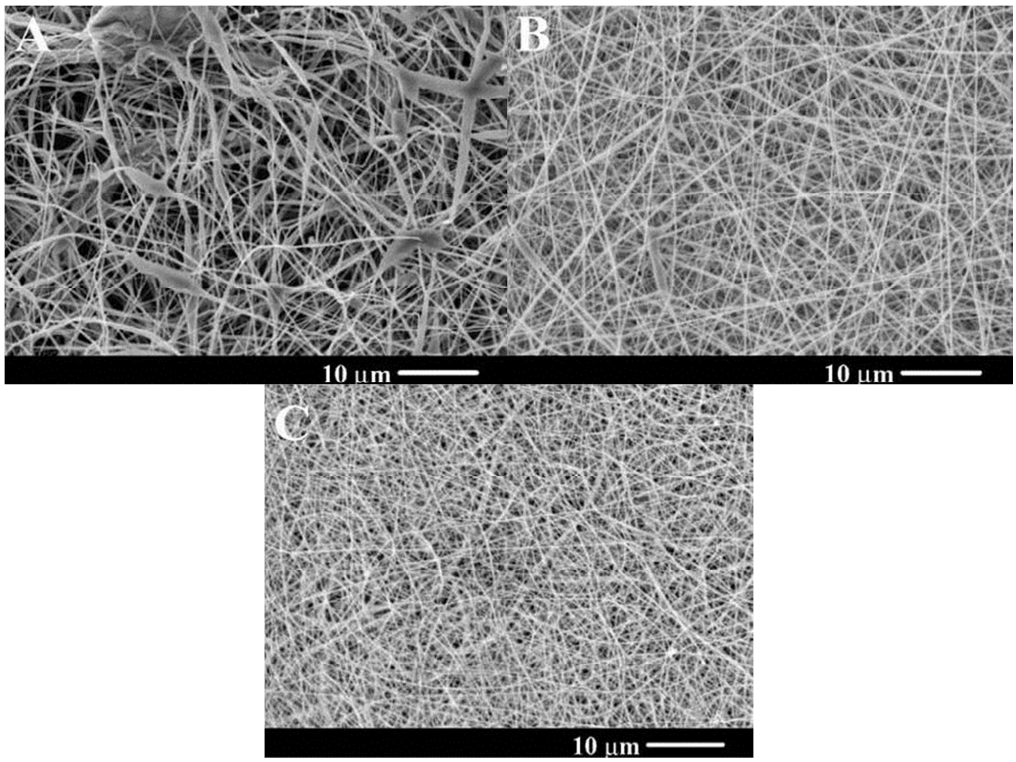


***Figure 10 –*** *SEM images for electrospinning scaffolds of PDLA in the presence of different salts (a) $KH_2PO4$, (b) $NaH_2PO_4$ and (c) NaCl, this last more conductive and so resulting in a substrate with fewer defects* **[31]**.

The first one,is reported to decrease fiber diameter with increasing electrospinning voltage [12]. Although differently Zong [31] and Chung [32] have observed the opposite influence, i.e. the higher voltage, the larger the fiber diameter, for electrospinning of PDLA and PLCL (50:50) respectively (*Figure 11*).

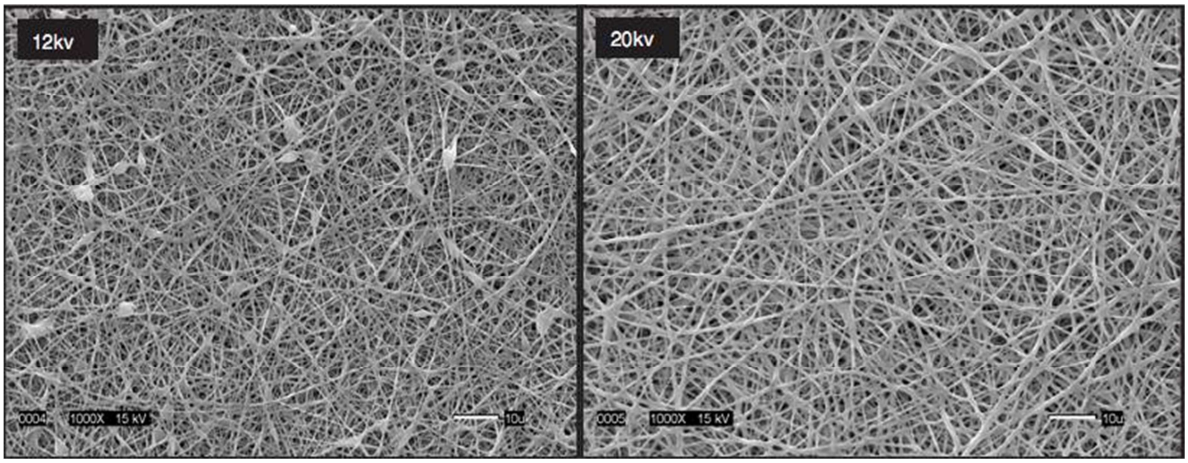


***Figure 11 –*** *Applied voltage influence on fiber diameter in electrospinning of PLCL (50:50) concentration of 12% in acetone for (a) 12KV and (b) 20KV* **[32]**.

Deitzel [22] produced nanofibers of poly(ethylene oxide) (PEO) and evaluated the influence of the voltage on the final morphology of the scaffold. According to the study, increasing the voltage causes the rate at which solution is removed from the tip to exceed the flow rate, resulting in a less stable jet. Therefore, fiber bead density increases with the increasing instability of the jet and the increasing of applied voltage. Again, a different opinion was given by Wannatong [26] that believes that increasing the applied potential bead formation became less probable.

The second process parameter is the flow rate of the solution, controlled by the injection pump. For lower flow rates fibers with smaller diameters are formed and for too high flow rates it is noticed the presence of beading, thicker nanofibers and irregularities, since the amount of solution is too big for the jet to carry [28, 32] and fibers do not have the chance to dry before reaching the collector [31]. To achieve a more stable jet a minimum of flow rate should be used [28] paying attention to the possible formation of beading for very slow flow rates as noticed by Chung [32].

In order to guaranty the complete evaporation of the solvent and prevent the formation of beads and junctions in the membrane [22, 31], it is necessary to adjust the distance between the needle and collector. This parameter is responsible and influences the flight time of the jet, and so the final morphology due to the presence or not of solvent in the structure [28].

As for the environmental parameters, humidity can also cause changes in the fiber morphology. The humidity does not show an effect on fiber diameters or shape, but instead changes the porosity of the fibers – more humidity higher the porosity of the fiber [28, 35]. Casper [35] studied this effect in the electrospinning of a solution of PS and tetrahydrofuran (THF), varying the humidity next to the region of process.

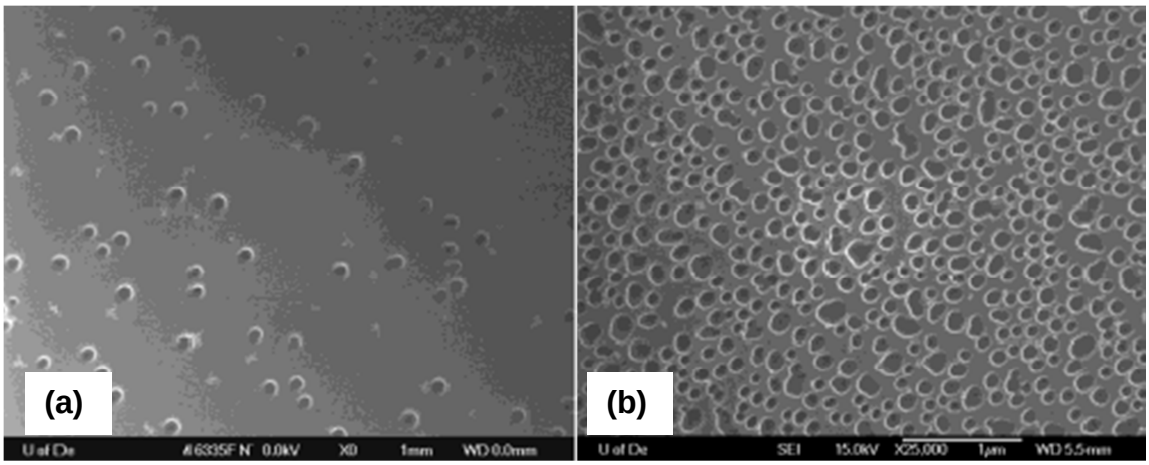


***Figure 12 –*** *SEM images of the effect of humidity in the porosity of fibers of PS, when (a) 40-45% and (b) 50-59% of relative humidity is used* **[35]**.

To summarize all the parameters mentioned above must be adjusted to produce a uniform nanofiber defect free scaffold by electrospinning, but this ideal situation is hard to be achieved [7, 19]. Typically, a trial-and-error approach has been used in which the solution properties and electrospinning parameters are varied until desired scaffold is obtained [14].

### 1.3.2. Different setups and fiber alignment

The electrospinning process allows the preparation of a non-woven nanofiber scaffold. Because of the bending instability, the alignment of fibers requires specific set ups [19 (*Figure 13*) that induce the orientation of the fibers in the scaffold.

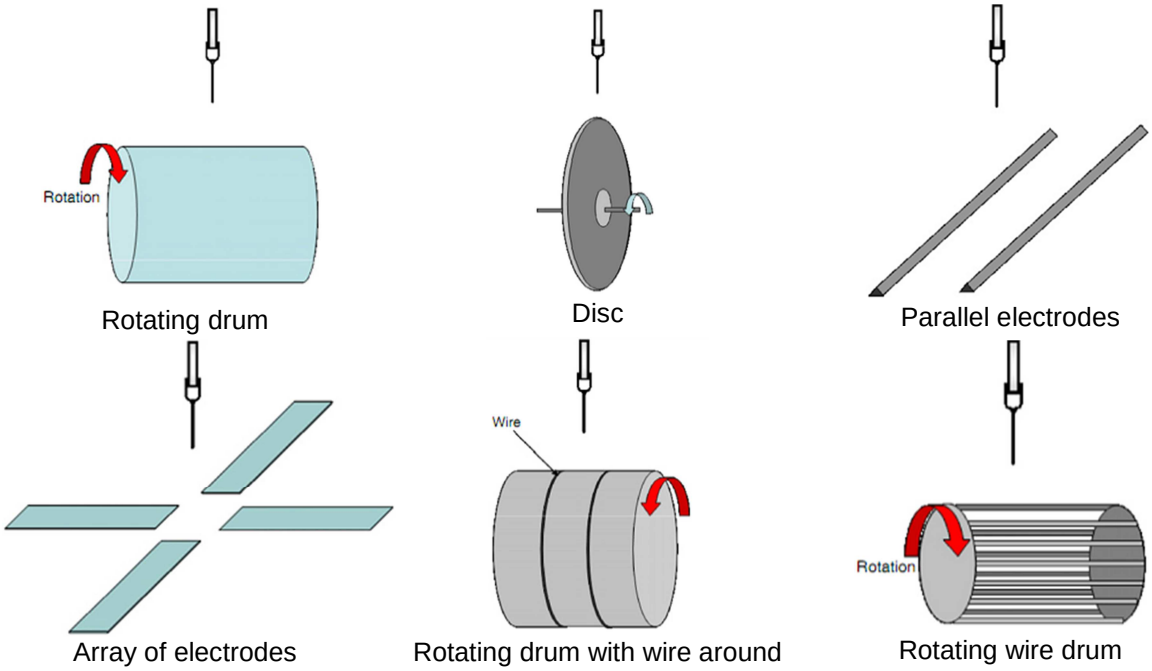


***Figure 13 –*** *Examples of different setups for electrospinning (Adapted from* **[21]***).*

The simplest one is the use of a rotating drum that includes another process parameter, the rotation speed. The rotation speed determines the fiber alignment, i.e. the faster the rotation speed more aligned are the fibers (*Figure 14*) [7, 26, 32, 36]. It was observed that fiber diameters did not change with the variation of rotational speed [26] and there is a limit before fibers suffer fracture [36].

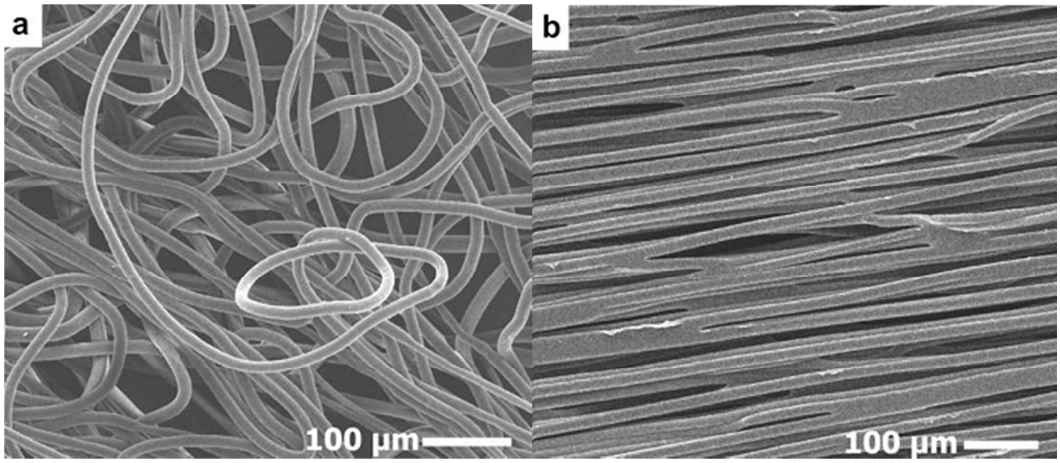


***Figure 14 –*** *Electrospinning of PCL in (a) planar collector and (b) rotational drum* **[36]***.*

### 1.3.3. Advantages and applications

As explained before, it is desirable to design a scaffold with mechanical and biological properties similar to ECM in order to best modulate cellular behavior [14]. That includes the morphology of the scaffold, since the topography will affect cell behavior [15]. Therefore, the main advantage of electrospinning is the possibility of produce a scaffold formed by fiber in the nanoscale, the same magnitude of ECM [14, 19, 23], which favors cellular response, including adhesion, proliferation and maintenance [37]

Decreasing the fiber diameter scale, the substrate will have a high surface area, flexibility on surface functions and better mechanical properties [7, 19]. In addition, compared to other techniques, electrospinning is a simpler and less expensive way to produce scaffolds [14, 28, 37].

A variety of materials may be processed by electrospinning, including natural polymers and temperature sensitive materials, such as enzymes and biological substances that may lose their functionality if temperature is applied [28]. In addition, electrospinning allows the use of many synthetic and natural polymers, as well as combining inorganic materials, additives and biomolecules to adjust the scaffold to a specific application

The biomedical applications of electrospinning nanofibers include tissue engineering scaffolds, such as cartilage, bone, nerve, wound dressing, heart tissue and blood vessel; anti-adhesion membrane; drug delivery systems and biocatalyst [14, 28, 31, 37]. Due to its high surface area and interconnected pores, the electrospun scaffold is adequate to tissue growth. Other applications of electrospinning not in the biomedical field are filters, biosensors, cosmetics and protective clothing [19, 37].

## 2. OBJECTIVES

The electrospinning technique allows the production of nanofiber scaffolds, i.e. substrates with fiber diameter in the same order of magnitude of the extra cellular matrix (ECM), and allows a better cellular adhesion, growth and proliferation. This characteristic morphology together with the high porosity and surface area makes the process useful in many applications, among them the medical field, since the biocompatible and biodegradable polymers can be processed

Thus, this study aimed to process by electrospinning the copolymer poly(L,L-lactide-ε-caprolactone), varying parameters such as concentration, flow rate, applied voltage and distance between needle and collector in order to obtain a nanostructured scaffold. The membranes obtained were physical and mechanical characterized, as well as seeded with aortic valve cells to verify its biocompatibility.

Proposed objectives for this work are:

- identify the process parameters to perform the electrospinning of poly(L,L-lactide-ε-caprolactone);
- produce a nanostructured scaffold;
- characterize its surface in terms of morphology, uniformity and presence of defects;
- characterize the mechanical properties of the substrate, namely perform the tensile test and tear resistance tests;
- verify the cell adhesion and proliferation within the scaffold, through the observation by confocal microscope and SEM;
- quantify the viable cells within the substrate during cultivation, using MTT assay.

# 3. EXPERIMENTAL

## *3.1. Materials*

The copolymer poly (LL-lactide-ε-caprolactone) (60:40) (PLCL) was synthesized in the laboratory of Macromolecules Engineering of the Department of Metallurgical and Materials Engineering (Escola Politécnica da Universidade de São Paulo, EPUSP) as described by [11]. A few properties of PLCL are summarized in *Table 5*.

***Table 5 –*** *Summary of few properties of PLCL.*

| | $T_g$ ($^oC$) | $T_m$ ($^oC$) | Crystallinity (DSC) (%) |
|---|---|---|---|
| PLCL | -24.87 | 104.38 | 9.95 |

Commercially available polylactide (PLLA) PURASORB PL was purchased from Purac. Its physical properties are shown in *Table 6*.

***Table 6 –*** *Physical properties of PURASORB PL.*

| Young's modulus (GPa) | Elongation (%) | Tensile strength (MPa) | Density ($g/cm^3$) | $T_m$ ($^oC$) | $T_g$ ($^oC$) | Degradation time (months) |
|---|---|---|---|---|---|---|
| 3-5 | 3-6 | 50-60 | 1.25-1.30 | 170-200 | 55-65 | >24 |

Solvents, solutions and dyes used in this work are listed below:

- Chloroform ($CHCl_3$), 99-99.4% of purity, purchased from MERCK;

- Dimethyl sulfoxide ($C_2H_6SO$) (DMSO), purity higher than 99.9%, purchased from SIGMA-Aldrich (D8418);
- Dulbecco's Modified Eagle's Medium (DMEM) purchased from Invitrogen-Gibco;
- Tripan blue purchased from SIGMA-Aldrich (T6146);
- Hoechst 33342, purity higher than 98%, purchased from SIGMA-Aldrich;
- 3-[4,5-dimethylthiazol-2]-2,5-diphenyltetrazolium bromide (MTT), purity of 97.5%, purchased from SIGMA-Aldrich.

## *3.2. Production of scaffold*

The scaffolds were obtained through the process of electrospinning, , of PLLA:PLCL in different proportions and concentrations. Briefly, the apparatus is consisted by a high voltage source, a metal collector (plane or rotating) and an injection pump (Harvard Apparatus 901) to control the solution flow rate; the pump is connected to a syringe with a metal needle with a diameter of 1.8mm (*Figure 15*).

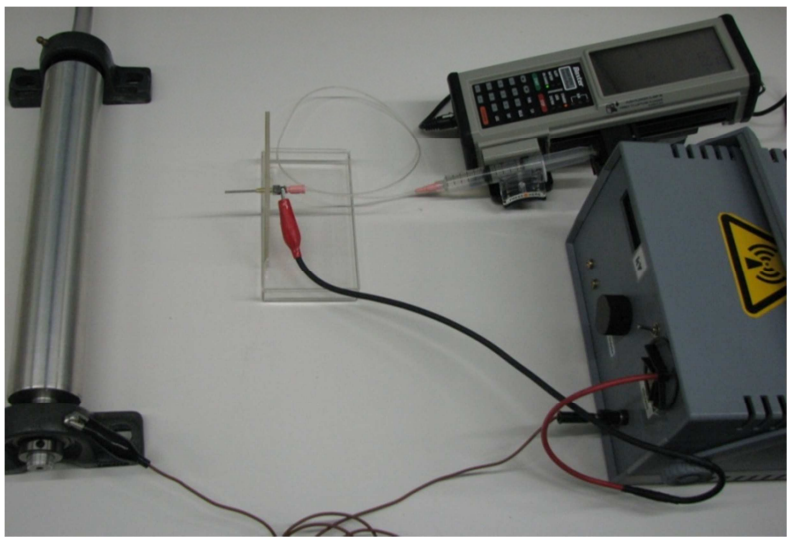

***Figure 15 –*** *Electrospinning apparatus.*

The distance between collector and tip of the needle, voltage applied and solution flow were varied until electrospinning was successfully performed, i.e. uniform fibers were obtained. As well as the process parameters, the solution concentration and proportion between the polymers varied during the experiments. It was used a plane square collector wrapped in aluminum foil[4] to remove more easily the substrate. After choosing the most adequate condition, all the parameters were finally fixed and the final scaffold produced.

## *3.3. Characterization*

### 3.3.1. Differential scanning calorimetry (DSC)

Differential scanning calorimetry measures the variation of the heat flow in a sample compared to a reference, while subjected to a temperature scanning at controlled constant rate. By this analysis it is possible to observe the thermal transitions of the sample, such as melting temperature ($T_m$), glass transition ($T_g$) and crystallization transition ($T_c$).

The temperature ranged from -80$^o$C to 210$^o$C, at a rate of 20$^o$C per minute, and nitrogen flow of 50mL/min. Graphics of heat flow versus temperature were acquired and percentage of crystallization of the material was calculated according to *Equation 1*, where $\Delta H_m$ = melting enthalpy (J/g), 93 and 142 are the melting enthalpy (J/g) for PLLA and PCL 100% crystalline respectively, and c = concentration (%) of PLLA or PCL.

[4] The aluminum foil used to collect nanofibers should be wrinkle-free since the wrinkled surface may result in uneven fiber deposition [7].

$$crystallization(\%) = \frac{100.\Delta H_m}{93.c_{PLLA} + 142.c_{PCL}}$$

***Equation 1 –*** *Calculation of the percentage of crystallization.*

### 3.3.2. Surface characterization

Scanning electron microscopy (SEM) (Philips XL30) was used to check the fiber formation and observe the defects and morphology of the fibers. Prior to the analysis, the samples of the scaffolds were coated with gold.

Images obtained by SEM were used to verify the range of fiber size obtained, i.e. the diameter of various fibers was measured in order to verify its magnitude. However, no statistical analyses were made.

### 3.3.3. Tensile testing

The tensile properties of the scaffold were measured using nine test specimens as *Figure 16* with the dimensions W= 15mm, H= 38mm, w= 5mm and h= 22mm, in a tensile testing machine from INSTRON model 5565 (*Figure 17*). The specimens were cut paying attention to prevent flaws and tears formation that could cause premature failure of the scaffold. A 10kg load cell was used and the cross-head speed was set at 1mm/min. No conditioning procedure was previously made.

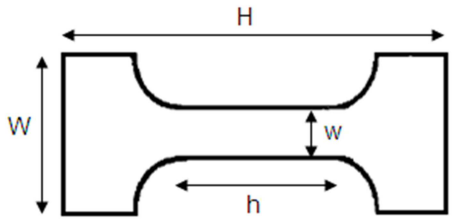


***Figure 16 –*** *Test specimen for tensile testing.*

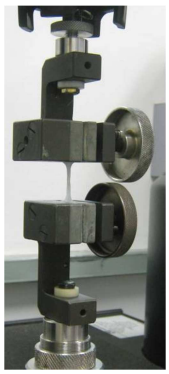

***Figure 17 –*** *INSTRON 5565 from Material Department of "Faculdade de Odontologia" from USP – FOUSP.*

Results were obtained as force (F) and variation of the gage length (ΔL), and the curve stress (σ) versus strain (ε) was calculated using Equation 2 and 3, where A = area, t = thickness and $L_0$ = initial gage length of the sample.

$$\sigma = \frac{F}{A} \; and \; A = w.t$$

***Equation 2 –*** *Calculation of stress (MPa).*

$$\varepsilon = \frac{\Delta L}{L_o}.100$$

***Equation 3 –*** *Calculation of strain(%).*

### 3.3.4. Tear Resistance

The tear resistance test was also realized in INSTRON 5565, but the test specimens (5 samples) were cut according to *Figure 18*, where H= 75mm, T= 50mm and W= 25mm. As well as in the tensile testing, no conditioning procedure was made; the load cell used was 10kg, an initial gap of 50mm and a cross-head speed of 5mm/min were set. Results were obtained as load (F) along the time (Δt).

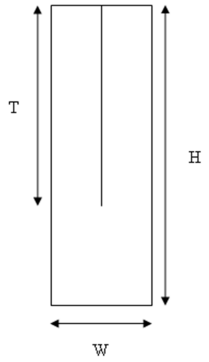


***Figure 18 –*** *Tear resistance specimen configuration.*

## *3.4. Cell Culture*

### 3.4.1. Growth and proliferation of cells

The porcine aortic valve cells (*Figure 19*) were given by the Bioengineering Laboratory in the Heart Institute (INCOR) from “Hospital das Clínicas” of the Universidade de São Paulo. The cells were maintained in flaks with culture medium DMEM containing 10% (v/v) fetal bovine serum and 1% (v/v) of penicillin streptomycin; in an incubator at 37$^{o}$C with 5% carbon dioxide in air. At confluence, cells were dissociated with trypsin by the standard protocol, i.e. remove the medium, wash with PBS (Phosphate-buffered saline), add trypsin and EDTA (Ethylenediaminetetraacetic acid), add DMEM for inhibition of trypsin and divide it into two flasks.

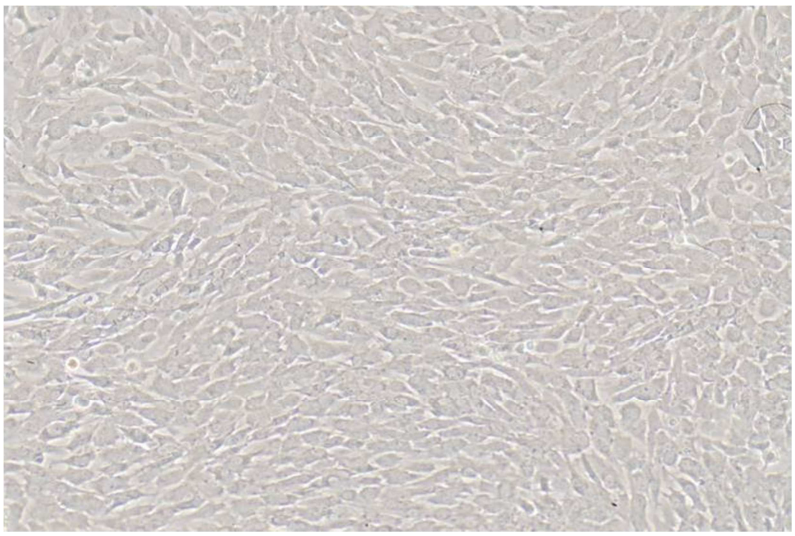

***Figure 19 –*** *Aortic valve cells at confluence at optical microscopy (10X).*

### 3.4.2. Seeding

Before seeding, scaffolds were disinfected in 70% (v/v) ethanol for more than 30 min and then washed with PBS to avoid traces of ethanol. In the meantime, the concentration of cells was calculated in order to guaranty that all the scaffolds were seeded with the same quantity of cells.

At confluence, cells were detached with trypsin as described before, the suspension centrifuged for 5min in 200G and then suspended in 1mL of DMEM. A sample of the final suspension was colored with Trypan blue – selectively vital stain that colors only the dead cells in blue – and observed in optical microscope assisted by a Neubauer chamber. The concentration of the cell suspension (C) was calculated as *Equation 4*, where N = number of non-colored cells counted; D = dilution made and V = volume of the chamber.

$$C = N.D.V$$

***Equation 4 –*** *Concentration of cell suspension.*

The scaffolds were then seeded and the plate completed with DMEM; the medium was replaced every 2 days and the culture was maintained in an incubator at 37$^{o}$C with 5% carbon dioxide in air up to 7 days.

### 3.4.4. Cell distribution and adhesion

A qualitative analysis was performed using a confocal laser scanning microscope (CLSM). Scaffolds samples were removed from the culture on different days and fixated with 4% paraformaldehyde for 10 min. Scaffolds were dried, then frozen with liquid nitrogen and maintained in -80$^{o}$C to preserve cell structure. On the day of observation, all samples were immersed in paraformaldehyde to rehydrate the cells and then washed with PBS. After that, they were submerged in 1mL of a 100:1 solution of PBS and Hoechst (1mg/mL); this last is a fluorescent dye that binds to DNA and so it enables the visualization of the nucleus of the cells. After 15 min, the samples were washed once more with PBS and then were mounted on glass microscope slides with glycerol and PBS (50:50), always maintained covered with aluminum to avoid lost in its fluorescence. Finally, samples were observed by the confocal laser microscopy (LSM510META – Carlzeiss).

Another observation was done by the scanning electron microscopy (SEM). For that purpose, a scaffold samples o day 4 of culture was taken and immersed for 30min in 4% paraformaldehyde to fixate the valve cells. The samples were observed in the microscope after their coating with gold. However, since SEM works under vacuum, it was necessary to dehydrate the cells before coating and observation. In order to do that and not cause any damage to the cell morphology, it was done a dehydration through a series of graded ethanol solutions (20, 40, 50, 70, 85 and 100%) for 20 min in each one and then air dried.

### 3.4.5. Viability of cells

Quantifying cells within a scaffold using visual observation can be difficult because of its lack of uniformity in the surface. Moreover it is necessary to guarantee the observation of a representative part of the substrate. Therefore, the MTT assay was chosen to quantify the viable cell within the scaffold. The technique is based on the conversion of the tetrazolium salt into formazan crystals done by the succinate-tetrazolium reductase system in the mitochondria of the metabolically active cells in the culture. The amount of formazan formed is directly correlated to the number of cells.

The procedure starts 4 h prior to the end of cultivation, when 20 μL of MTT (5 mg/mL) was added to each sample. It is noted that the medium was replaced by 200 μL of a fresh one, in order to remove the unattached cells. After those 4h of incubation, all the liquid was removed and 200 μL of DMSO was used to dissolve the crystals formed. The DMSO was left for 15 min under gentle agitation to guarantee that all crystals were dissolved. The solution was colorimetric analyzed (U1500 Spectrophotometer – Hitachi) at $\lambda$ = 570nm, using pure DMSO, as control since it was observed that there was no interaction of the biomaterial with the components. The results were expressed in absorbance versus time of culture.

# 4. RESULTS AND DISCUSSION

## *4.1. Electrospinning*

After assembling all components needed for electrospinning, it was necessary to find the optimal combination of the parameters for electrospinning. The parameters include process parameters such as distance between needle and collector, flow rate and applied voltage, as well as the concentration of the polymer solution and the solvent used. While the optimal combination is not achieved the substrate formed will contain defects, e.g. beads and larger diameters enlargements [7]. So, the performance of the process was verified by SEM, until definition of the parameters.

As viscosity is the main parameter for the fiber formation, this was the first parameter to be varied, until minimal intermolecular interaction was achieved, i.e. until viscosity is sufficient for allowing process to occur. This parameter is mainly controlled by the polymer concentration in the solution.

In order to successfully electrospin poly(L,L-lactide-co-ε-caprolactone) (PLCL), polymer solutions at 5%, 6%, 8% and 20% (*Table 7*) in acetone, chloroform or the combination of both were tested. Even though a few references were used as a starting point [12, 38-40], the variation of the parameters was made by trial-and-error approach, as normally done at this stage of process; after fixing the concentration to be used the influence of each parameter is used to establish the beneficial combination to obtain an uniform defect free nanofiber scaffold.

After several attempts at lower concentrations (*Figure 20*), it was decided to try a higher concentration (20%), since it was noticed that viscosity, or better yet, the polymer concentration was insufficient for fiber production.

***Table 7 –*** *Different parameters used for electrospinning of PLCL.*

| | Concentration (%) | Solvent | Voltage (KV) | Distance (cm) | Flow rate (mL/h) |
|---|---|---|---|---|---|
| (i) | 5 | AC | 9-15 | 12 | 1.236 |
| (ii) | 5 | AC | 12-15 | 12 | 3.06 |
| (iii) | 5 | AC | 18-20 | 12 | 1.236 |
| (iv) | 5 | AC | 18-20 | 15 | 1.236 |
| (i) | 6 | CLO | 15 | 12 | 1.236 |
| (ii) | 6 | CLO | 15 | 12 | 3.06 |
| X | 6 | CLO | 15 | 15 | 1.236 |
| X | 6 | CLO | 15 | 20 | 1.236 |
| (iii) | 6 | CLO | 20 | 12 | 3.06 |
| (iv) | 6 | CLO | 20 | 12 | 6.18 |
| X | 6 | CLO | 20 | 20 | 6.18 |
| (v) | 6 | CLO+AC | 9-15 | 12 | 1.236 |
| (vi) | 6 | CLO+AC | 9-15 | 12 | 3.06 |
| (vii) | 6 | CLO+AC | 15-18 | 12 | 3.06 |
| (viii) | 6 | CLO+AC | 15-18 | 12 | 12.36 |
| (ix) | 6 | CLO+AC | 20 | 12 | 3.06 |
| (i) | 8 | CLO | 15-18 | 12 | 6.18 |
| (ii) | 8 | CLO | 20 | 10 | 0.618 |
| X | 8 | CLO | 20 | 12 | 0.618 |
| (iii) | 8 | CLO | 20 | 12 | 1.236 |
| X | 8 | CLO | 20 | 13 | 1.236 |
| X | 8 | CLO | 20 | 15 | 1.236 |
| (iv) | 8 | CLO | 22 | 12 | 1.236 |
| X | 8 | CLO | 23 | 10 | 1.236 |
| (v) | 8 | CLO | 25 | 12 | 1.236 |
| X | 8 | CLO | 25 | 12 | 6.18 |
| X | 8 | CLO | 25 | 12 | 3.06 |
| X | 8 | CLO | 25 | 12 | 0.618 |
| X | 8 | CLO | 25 | 15 | 1.236 |
| (i) | 20 | CLO+AC | 13 | 12 | 3.06 |
| (ii) | 20 | CLO+AC | 13 | 12 | 1.236 |
| (iii) | 20 | CLO+AC | 15-18 | 12 | 12.36 |
| (iv) | 20 | CLO+AC | 15-18 | 12 | 3.06 |
| (v) | 20 | CLO+AC | 15-18 | 12 | 1.236 |
| (vi) | 20 | CLO+AC | 15-18 | 12 | 0.618 |
| (vii) | 20 | CLO+AC | 15-18 | 12 | 0.306 |
| (viii) | 20 | CLO+AC | 15-18 | 12 | 0.1236 |
| (ix) | 20 | CLO+AC | 20 | 12 | 3.06 |
| (x) | 20 | CLO+AC | 20 | 12 | 1.236 |
| X | 20 | CLO+AC | 20 | 12 | 0.618 |
| (xi) | 20 | CLO+AC | 23 | 12 | 3.06 |
| (xii) | 20 | CLO+AC | 23 | 12 | 1.236 |
| X | 20 | CLO+AC | 23 | 12 | 0.618 |

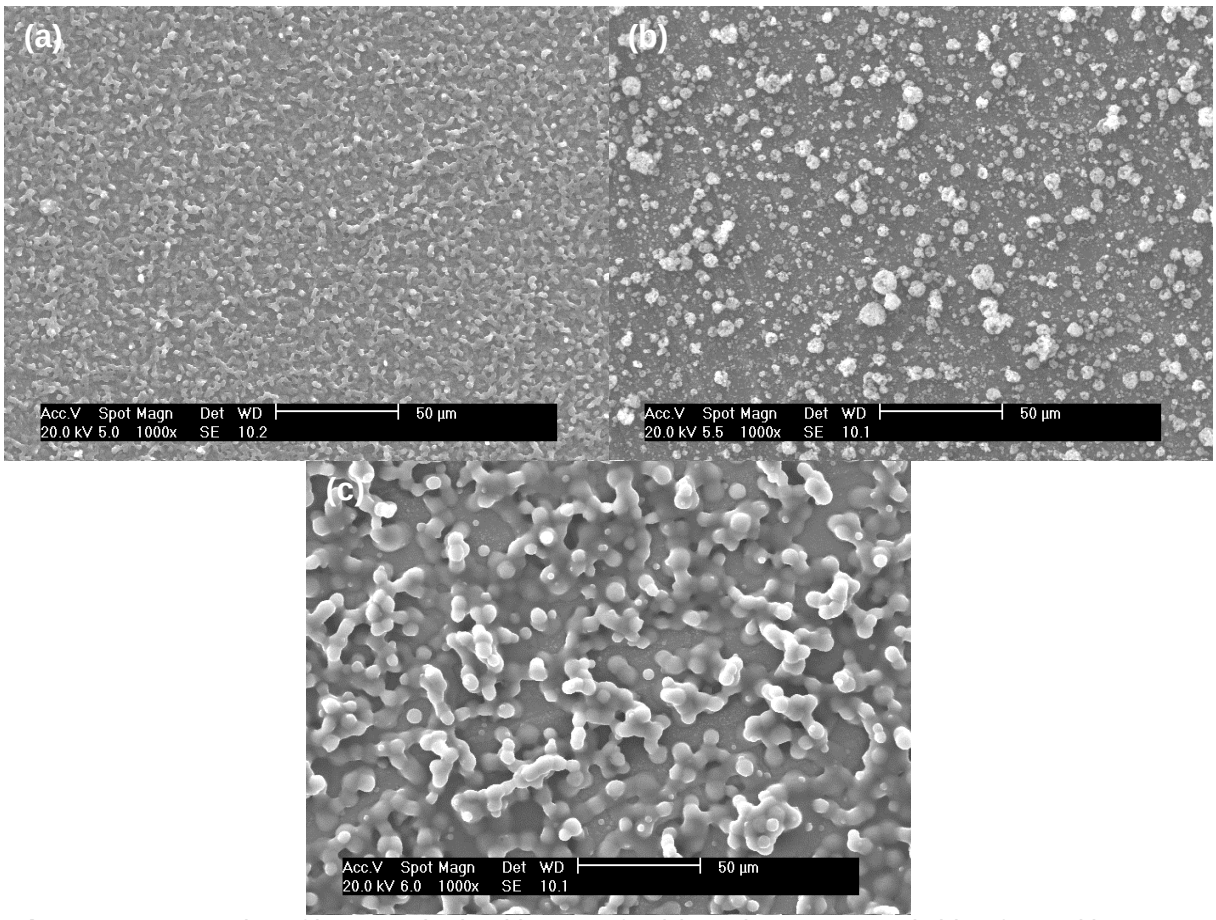


***Figure 20 –*** *Examples of images obtained by SEM for (a) 6% in acetone and chloroform with 9-15KV, 12cm and 1.236mL/h; (b) 5% in acetone using 18-20KV, 15cm and 1.236 mL/h; and (c) 6% in chloroform with 15KV, 12cm and 1.236mL/h.*

The more interesting images, where it was possible to see the beginning of fiber formation, were obtained for a concentration of 8 and 20% (*Figure 21*), and so more attempts were made varying the rest of the parameters. However, it was not possible to produce the desired scaffold. A hypothesis is the low molecular mass of the copolymer, resulting in a solution with low viscosity, making necessary a higher polymer concentration for the process. In fact, images as in *Figure 21* are obtained when concentration is still not sufficient for the electrospinning process [41].

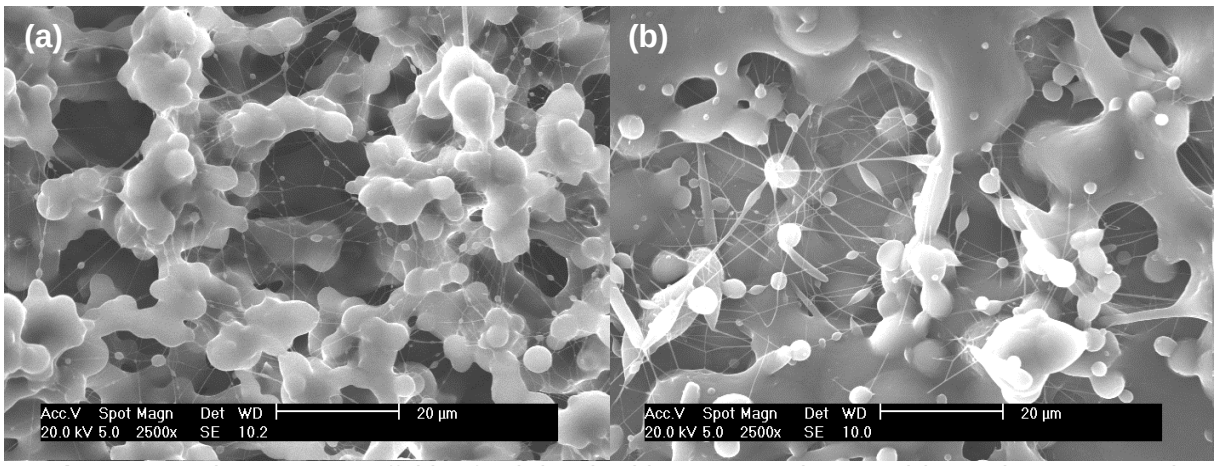


***Figure 21 –*** *Electrospun scaffolds of poly(L,L-lactide-co-ε-caprolactone: (a) 20% in acetone and chloroform with 15-18KV, 12cm, 3.06 mL/h and (b) 8% in chloroform using 20KV, 12cm, 1.236mL/h.*

At this point of the study, it was decided to blend the copolymer with poly(L,L-lactide) (PLLA) in order to increase the solution viscosity. The polymer choice was made based on the biopolymers well known for electrospinning, with higher molecular mass than PLCL to increase the intermolecular interactions. Moreover, it was chosen PLLA instead of PCL because of the slower degradation rate and worst cellular adhesion of PCL compared to PLLA.

The arrangement was necessary due not only the limited time available for the study but especially due the limited quantity of copolymer. So to proceed with the research and achieve its goals it was decided to continue doing the electrospinning of the blend.

Therefore, it was made several attempts with different proportions between PLCL and PLLA in different solution concentrations as seen in *Table 8*. For the electrospinning of the blend it was used as a start point literature references for the process of PLLA [42]. Attention was made to clogging at the tip of the needle, which happened often to (50:50) blend.

***Table 8 –*** *Different parameters used for electrospinning of PLLA:PLCL blend.*

| | | Concentration (%) | Solvent | Voltage (KV) | Distance (cm) | Flow rate (mL/h) |
|---|---|---|---|---|---|---|
| (i) | 50:50 | 5 | CLO | 17 | 7 | 3.06 |
| (ii) | 50:50 | 5 | CLO | 17 | 7 | 1.236 |
| (iii) | 50:50 | 5 | CLO | 17 | 7 | 0.618 |
| (i) | 30:70 | 5 | CLO | 17 | 7 | 3.06 |
| (ii) | 30:70 | 5 | CLO | 20 | 7 | 3.06 |
| (iii) | 30:70 | 10 | CLO | 20 | 10 | 3.06 |
| (iv) | 30:70 | 5 | CLO | 20 | 10 | 3.06 |
| (i) | 10:90 | 5 | CLO | 17 | 7 | 3.06 |
| X | 10:90 | 5 | CLO | 17 | 7 | 6.18 |
| (ii) | 10:90 | 5 | CLO | 17 | 10 | 6.18 |
| X | 10:90 | 10 | CLO | 17 | 7 | 3.06 |
| (iii) | 10:90 | 10 | CLO | 17 | 10 | 3.06 |
| (iv) | 10:90 | 10 | CLO | 17 | 10 | 1.236 |
| (v) | 10:90 | 10 | CLO | 20 | 10 | 3.06 |
| (vi) | 10:90 | 10 | CLO | 20 | 10 | 1.236 |

Comparing the substrate formed for different proportions of the blend, maintaining fixed the other parameters, it was possible to notice that higher percentage of PLLA allowed fiber formation. As observed in *Figure 22* when the proportion of (50:50) was used, fibers were formed; while for (30:70), it was possible to notice fibers besides many beads, demonstrating that viscosity was not high enough for a successful electrospinning; this observation applies even more for the (10:90) ratio.

Image (a) from *Figure 22* also shows the formation of a film, demonstrating that the amount of solution reaching the collector was higher than the electrical field could compensate, i.e. it was necessary to increase the applied voltage or decrease the flow rate. Since, the ideal is to use the lowest flow rate [28], and also it is preferable to use smaller voltages, the flow rate of the solution was decreased, making possible to visualize the influence of this parameter as well.

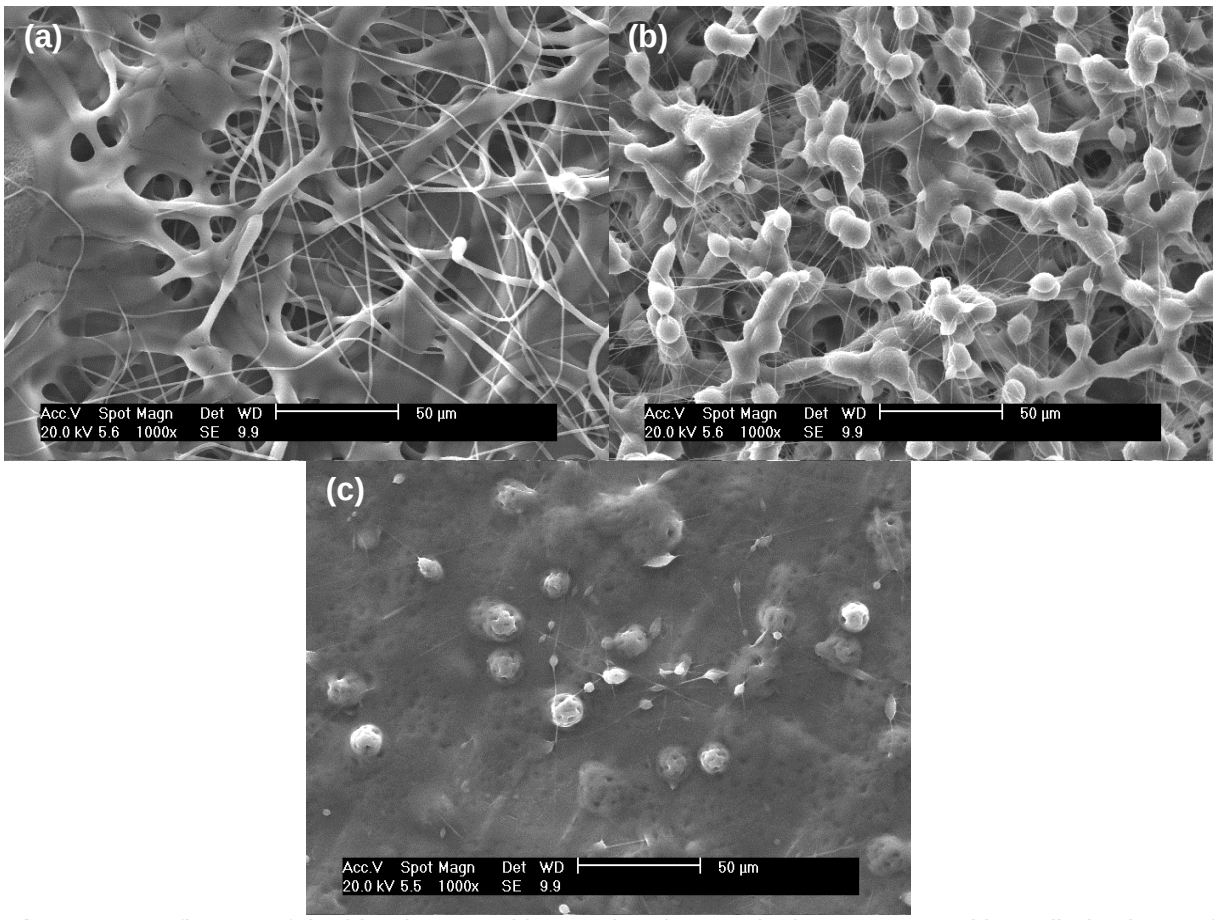


***Figure 22 –*** *Influence of the blend composition on the electrospinning process, with applied voltage of 17KV, distance between poles of 7cm and flow rate of 3.06mL/h. (a) (50:50), (b) (30:70) and (c) (10:90)*

The quality of the scaffolds changed dramatically with the flow rate, thus by decreasing the flow rate from 3.06 mL/h to 1.236 mL/h and then 0.618 mL/h, in scaffolds shown in *Figure 22* (a) and *Figure 23*, respectively were obtained. Not only smaller flow rates did not allow the film formation, but also allowed the formation of a fibrous scaffold with no beads or diameter enlargements. Moreover, the results sustained the influence of the flow rate seeing in literature; for smaller rates the fiber diameter decreases.

A last observation is the variation of fiber diameter within the scaffold. In *Figure 23* (a) the range of fiber diameter is around 2.11-3.21µm and for *Figure 23*(b) 1.54-3.07µm. Therefore, the scaffold with flow rate of 1.236mL/h resulted more uniform, compensating the larger diameters.

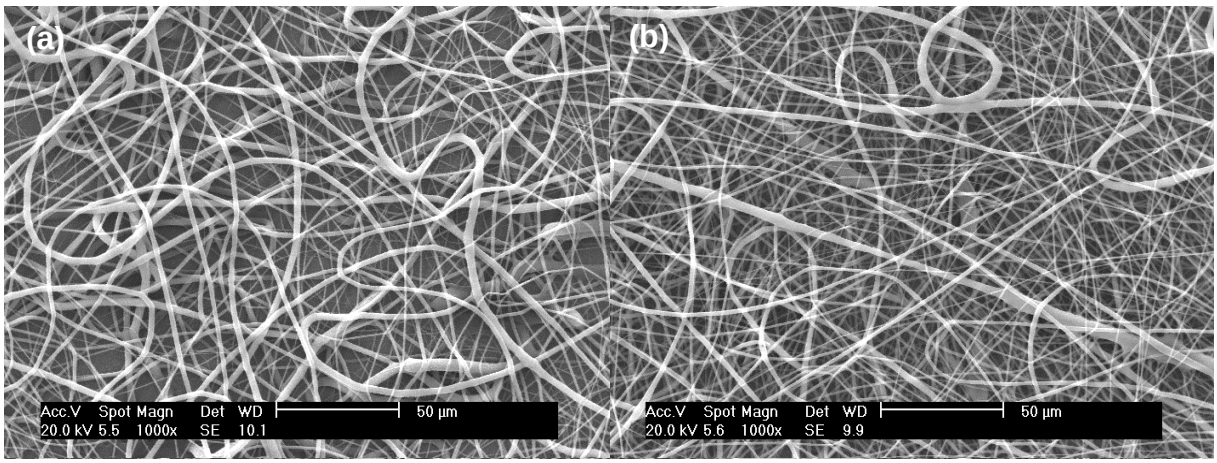


***Figure 23 –*** *Scaffolds obtained for (50:50) blend with concentration of 5% with different flow rates (a) 1.236mL/h and (b) 0.618mL/h.*

Aiming to decrease the fiber diameter in order to obtain a nanofiber scaffold, the study turned back to blends with smaller quantities of PLLA. As seen in *Figure 22* (b) and (c) the viscosity was not sufficient for the process, so in that case, the polymer solution was increased from 5% to 10%. *Figure 24* shows a substrate formed from a higher concentration solution; it is noted that the applied voltage and distance between needle and collector changed from the previous images.

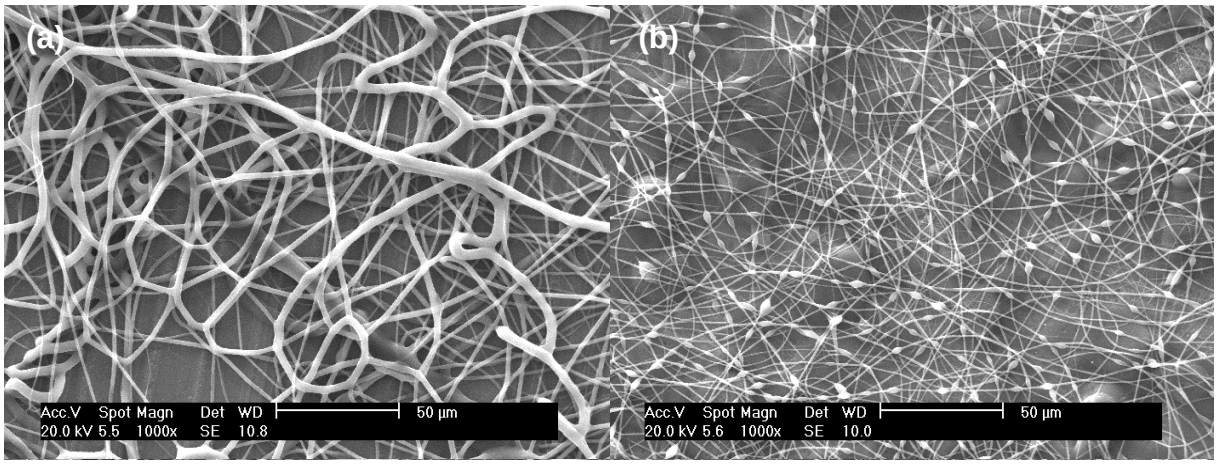


***Figure 24 –*** *Images for blend of (30:70) (a) 10% and (b) 5%; and parameters of 20KV, 10cm and 3.06mL/h.*

As expected, increasing the concentration of the solution the diameter of the fibers increased as well – the range of the fiber diameter went from 1.04-1.8µm to 1.68-3.89µm. Furthermore, for smaller concentrations the presence of defects was

increased. It is, then, possible to say that the effect caused by the variation of blend proportion and the polymer solution concentration is similar, since, blends of (30:70) and (10:90) presented a less uniform scaffold (*Figure 25*).

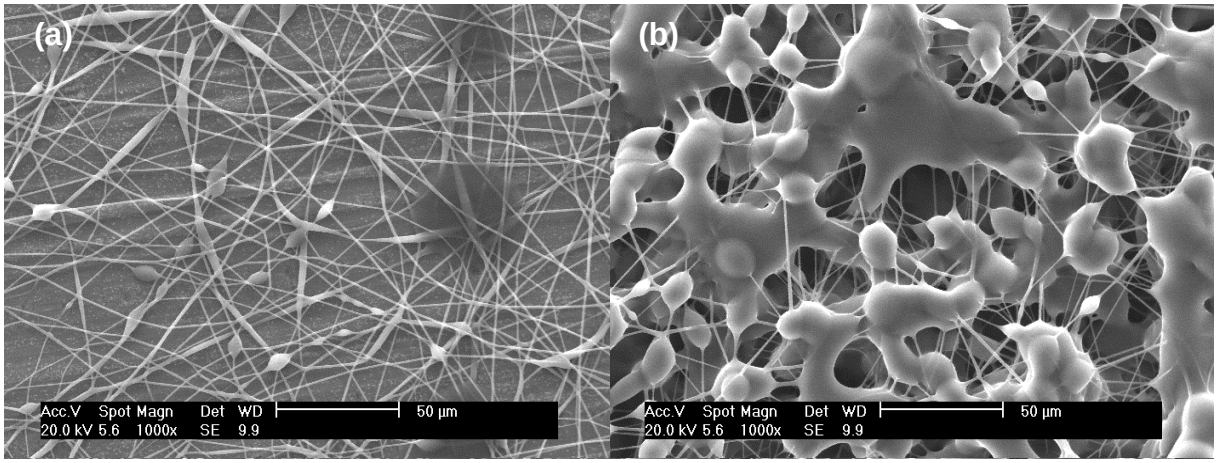


***Figure 25 –*** *Electrospinning scaffolds obtained from (10:90) (PLLA:PLCL) 10% both from the same membrane but different areas.*

Because of the lack of uniformity in the scaffold, it is hard to evaluate the effect of the other parameters, since different areas had different morphologies in the same scaffold. When electrospinning (10:90) (PLLA:PLCL) 10%, the increment of voltage introduced instability to the jet, increasing the number of defects (*Figure 26*).

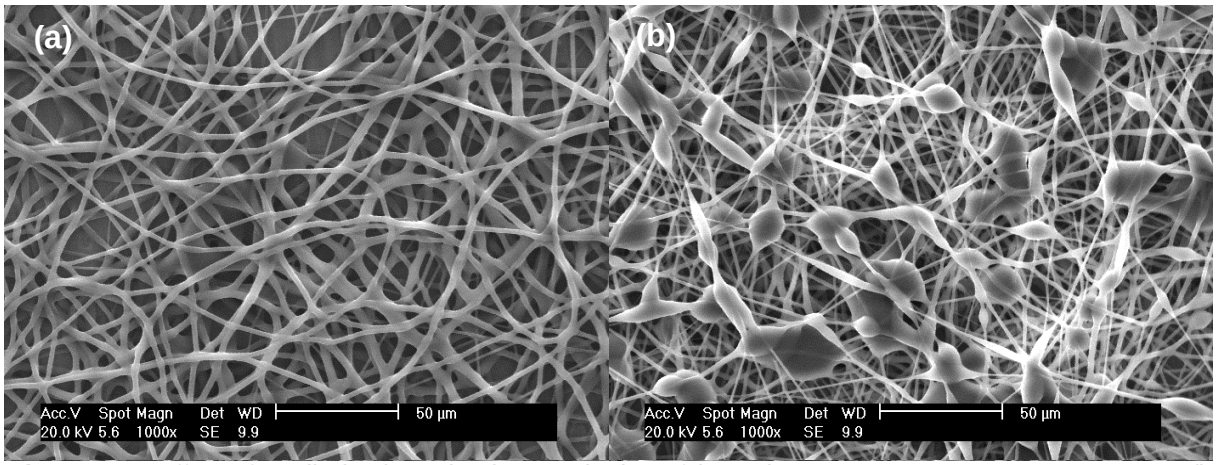


***Figure 26 –*** *Effect of applied voltage in electrospinning of (10:90) PLLA:PLCL 10%, 10cm, 1.236mL/h and (a) 17KV and (b) 20KV.*

On the other hand, when processing blend of (30:70) 5%, higher voltage induced the formation of a more uniform scaffold, with less beads and a small range of fiber diameter (*Figure 27*).

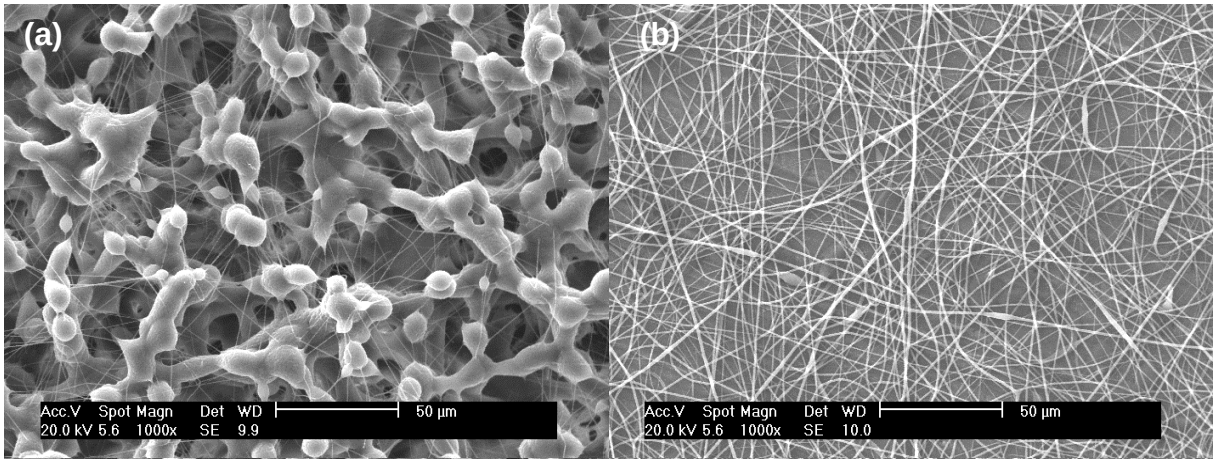


***Figure 27 –*** *Effect of applied voltage in electrospinning of (30:70) PLLA:PLCL 5%, 7cm, 3.06mL/h and (a) 17KV and (b) 20KV.*

These results may indicate that the influence of voltage is related to the viscosity of the solution, i.e. for lower viscosities increasing the voltage, and so the electrical forces, provokes the instability of the jet, and therefore the formation of defects. On contrary, solutions with higher viscosities are capable to compensate higher forces, and the effect is more uniform fibers with smaller diameter. However, this is just a hypothesis and further experiments with a more stable process and measurement of viscosity should be done to verify it.

Finally, it was decided to continue the study with the production of scaffolds by electrospinning PLLA:PLCL (50:50) 5% using the following process parameter: 17KV (applied voltage), 7cm ( distance between the poles) and 1.236mL/h (flow rate). The production of large scaffolds, necessary for further characterization, was done using a rotational collector, instead of the plane collector previously used. The rotation rate was kept low, around 6rpm, in order to enlarge the collector area and still allow random fiber deposition.

The parameters were chosen based, firstly, on the uniformity of the obtained scaffold; it is important to obtain a substrate with similar morphology in its whole area, otherwise its characteristics and cell culture results may not be coherent. Also, the membrane produced in these conditions did not have a considerable amount of defects.

The fiber diameter, however, was not as small (in the nanoscale) as aimed, being in the micron magnitude (*Figure 28* a). For that purpose, further experiments should be done, including decreasing the concentration, increasing the voltage or even using a needle with a smaller radius [28].

This last, not considered previously, gained attention due to the clotting at the tip of the needle noticed when producing scaffolds for a longer period of time. An additional effect of using a thinner needle diameter is the smaller quantity of beads in the final structure [12].

A first attempt in this sense was made using a needle with 1.5mm of diameter; as a result it was observed less clotting at the needle and range of fiber diameter from 1.57 to 3.37µm (*Figure 28* b).

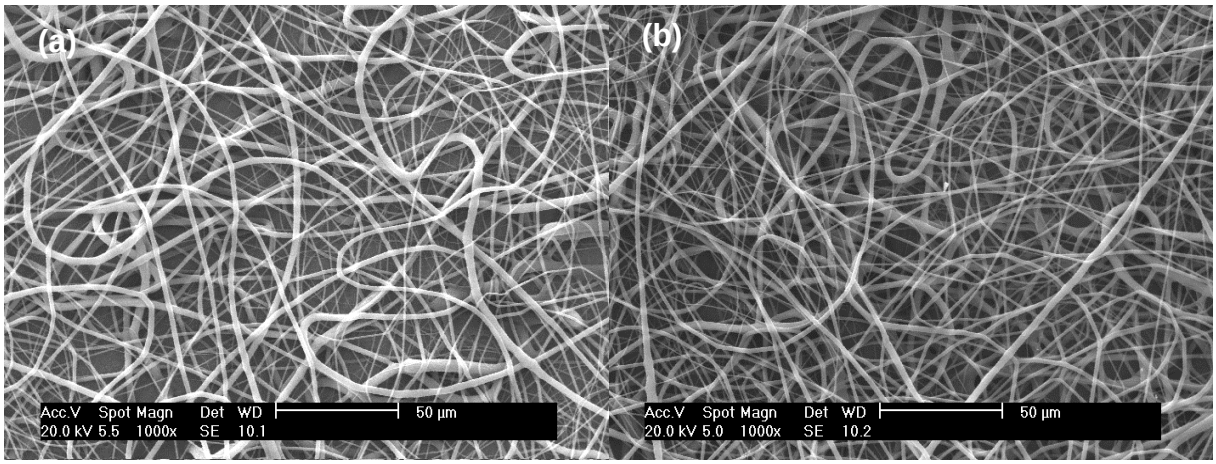


***Figure 28 –*** *Scaffold obtained from electrospinning of 5% (50:50) (PLLA:PLCL), parameters used 17KV, 7cm and 1.236mL/h , needle diameter of (a) 1.8mm and (b) 1.5mm.*

## *4.2. Scaffold characterization*

The characterization of scaffolds morphology was done using SEM during the whole procedure, as described in the last section, until achieving the desired fiber structure. So, just a few extra observations are relevant to point out in this section.

Firstly, during SEM analysis of the final substrate, the presence of few defects was noticed, that are basically agglomerations of fibers, as shown in *Figure 29*. Besides that, it was not observed any other defect, such as beads and diameters enlargements.

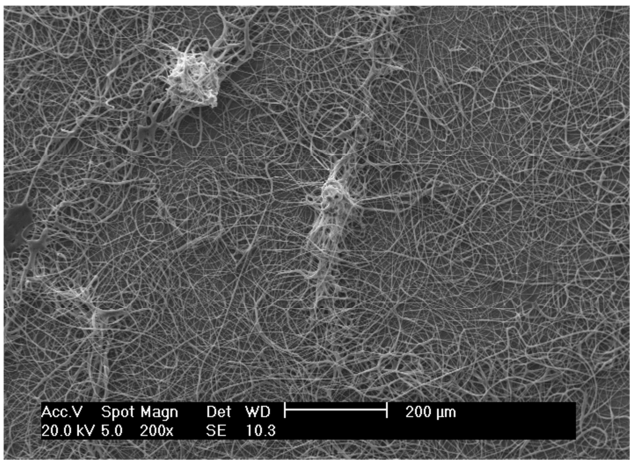


***Figure 29 –*** *Defect present in the final scaffold.*

Secondly, it was possible to observe the presence of porosity in the formed fibers (*Figure 30*); according to [28] and [35] due to humidity, since this environment parameter has been found to affect the surface morphology of fibers.

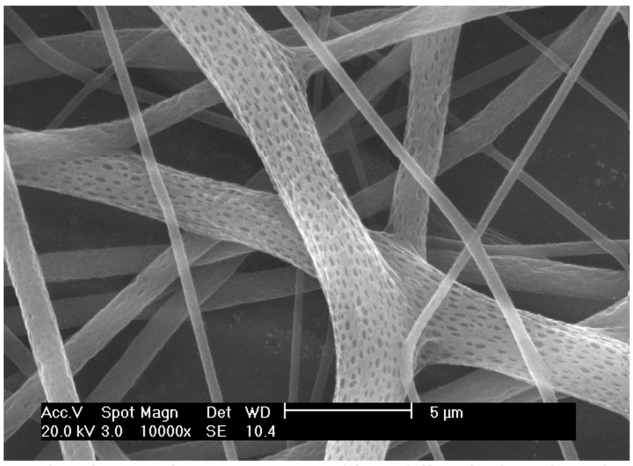


***Figure 30 –*** *Fiber porosity due to the presence of humidity during the electrospinning process.*

### 4.2.1. DSC

The DSC curves from the first heating for different electrospun scaffolds (*Figure 31*) were very similar, since they were produced from the same materials (supported by the second heating curves, that represent the material properties). However, it is interesting to observe a displacement of the PLLA melting temperature, $T_{m2}$, to higher temperature when blends having lower PLLA content (10:90 and 30:90) are compared to the (50:50) blend, while the cold crystallization temperature presented the opposite behavior. This can be explained by phase separation and crystallization induced by higher concentration of PLLA, leading to more stable crystallites.

The same effect can be observed comparing the results for PLCL only to those from the blend (50:50) (*Figure 32*). The blend (50:50) presented a higher $T_{m2}$, 173.5$^{o}$C, due to the presence of PLLA. The inhibition of the crystallization in copolymers is due to restrictions of the segmental motions and limitation of the phase separation of the different segments, lactide and caprolactone [44, 45].

In *Figure 31* results for the first heating are displayed and when comparing substrates having fibers with different diameters, such as 50:50 (b) and (c), it was not

possible to notice a difference in crystallinity between the scaffolds, and so the fiber diameter in this case did not affect the morphology.

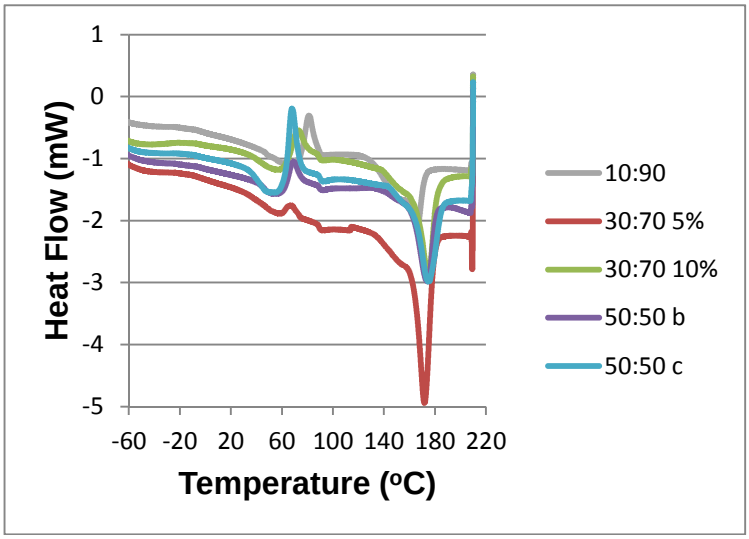


***Figure 31 –*** *Results of DSC analyses for different scaffolds produced by electrospinning in different proportions of PLLA:PLCL.*

Comparing the results for the first and the second heating for the electrospun scaffold (*Figure 32*), it is noted that $T_c$ was smaller for the first (69.5$^{o}$C) compared to the second (93.3$^{o}$C), this means that $T_c$ decreased when the material is electrospun, since the second heating refers to the blend itself. This fact may be related to the short period of time that the polymer had to solidify when being electrospun, i.e. the polymer once in solution travels a small distance to the collector and the solvent is completely evaporated, and so the time for the crystallization is short.

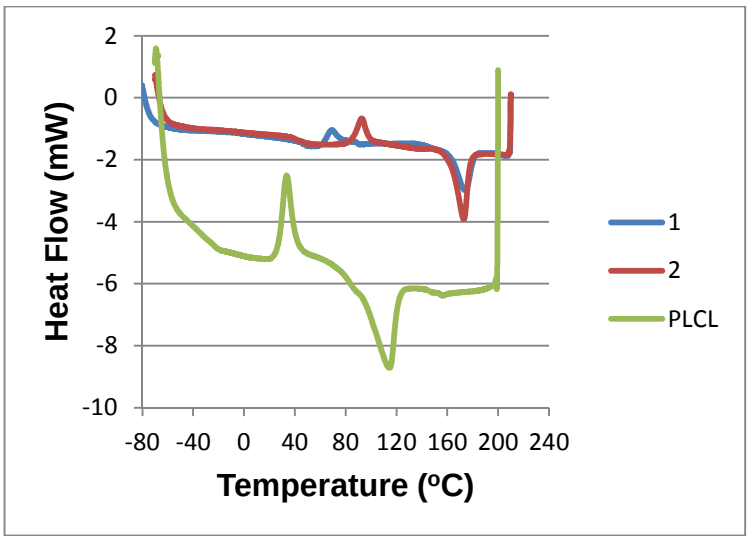


***Figure 32 –*** *Results of DSC for electrospun scaffold 50:50 PLLA:PLCL first and second heating and for PLCL unprocessed.*

Finally, crystallinity increased when PLLA was added to PLCL, reaching 30%; higher crystallinity was observed for blends with lower concentration of PLLA. *Table 9* summarizes the results; $T_{m1}$ and $T_{m2}$ refer to the melting temperatures of poly(ε-caprolactone) crystallites in PLCL and PLLA, respectively.

***Table 9 –*** *Results of DSC analyses.*

| | $T_{m1}$ (°C) | $T_c$ (°C) | $T_{m2}$ (°C) | $\Delta H_m$ (J/g) | Crystallinity (%) |
|---|---|---|---|---|---|
| 10:90 | 64.8 | 80,5 | 166.4 | 28.90 | 30.43 |
| 30:70 5 | 56.6 | 68 | 172.5 | 28.81 | 29.14 |
| 30:70 10 | 56.6 | 71.8 | 175.3 | 27.25 | 27.56 |
| 50:50 b | 54.5 | 69.5 | 174.3 | 24.72 | 24.05 |
| 50:50 c | 52.5 | 68.1 | 174.9 | 27.36 | 26.61 |
| PLCL | | 33.6 | 114.5 | 11.20 | 9.95 |

### 4.2.2. Tensile testing

For tensile properties characterization of a biomaterial scaffold, the ASTM F2150 standard suggests the use of several test methods, according to the scaffold's

physical and dimensional characteristics. Among them, the D1708 was used as reference, due to the thickness and dimensions of the specimens. However, the substrate produced by electrospinning is very thin and fragile, and so adaptations were made to allow the evaluation of the properties.

The tensile test was performed on 9 specimens with thickness in the range of 0.065 to 0.08mm – except one with 0.055mm. All cut from the same membrane. *Figure 33* shows part of the specimens after the test.

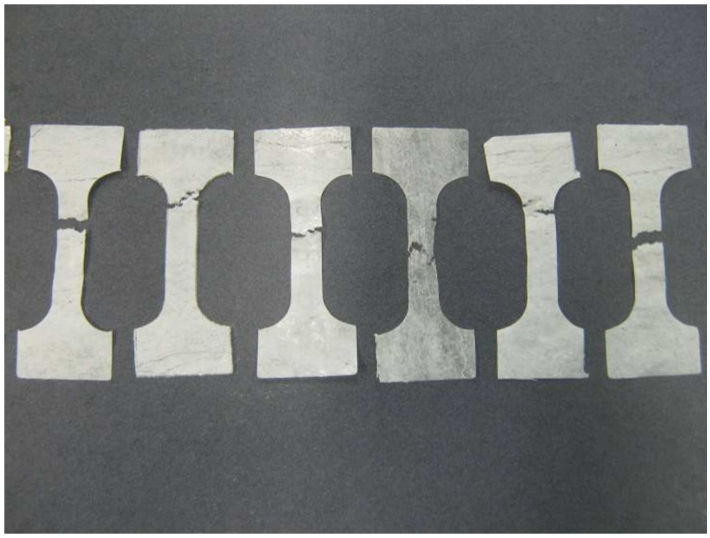

***Figure 33 –*** *Photography of test specimens after the tensile testing.*

The results obtained for each test specimen are seen in *Figure 34*. As could be expected for porous substrates, the curves presented variation among them; pores are defects in the structure and so, other than decreasing area supporting the applied load, they are responsible for stress concentration, decreasing the reproducibility of the test, since its distribution changed from a sample to another, i.e. it is not possible to assure that samples obtained by electrospinning have an equally pore distribution within the whole scaffold.

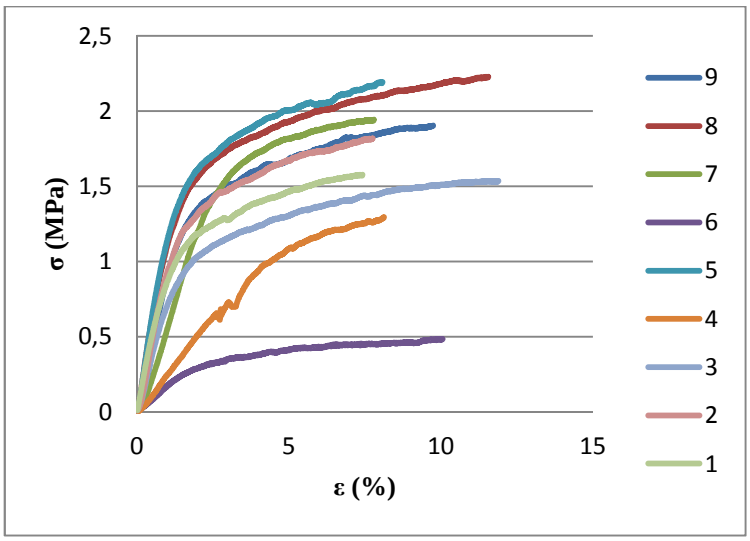


***Figure 34 –*** *Stress (MPa) X Strain (%) curve for membranes with 5% in concentration of PLLA:PLCL(50:50) produced by electrospinning.*

As pointed out before, one of the specimens had a smaller thickness compared to the rest; that was specimen number 6, which result largely differs from other samples. Therefore, it is clear that the thickness influences the final result; however it was not possible to correlate this parameter to the stress supported.

The maximum strain (ε) and stress (σ) before break for each specimen are in *Table 10*. The average is 9.04% and 1.81 MPa respectively, not considering the results for the specimen with thickness out of the determined range.

***Table 10 –*** *Results of maximum strain (ε) and stress (σ) before failure and average for specimens tested.*

| ε (%) | σ (MPa) |
|---|---|
| 7.42 | 1.58 |
| 7.76 | 1.82 |
| 11.89 | 1.54 |
| 8.12 | 1.29 |
| 8.08 | 2.19 |
| 10.05 | 0.48 |
| 7.80 | 1.94 |
| 11.55 | 2.23 |
| 9.74 | 1.90 |
| 9.04±1.79 | 1.81±0.33 |

An interesting observation is the alignment of the fibers in regions next to the rupture during the tensile testing, as noticed in *Figure 35*, indicating that fibers tend to organize themselves promoting the elongation of the scaffold.

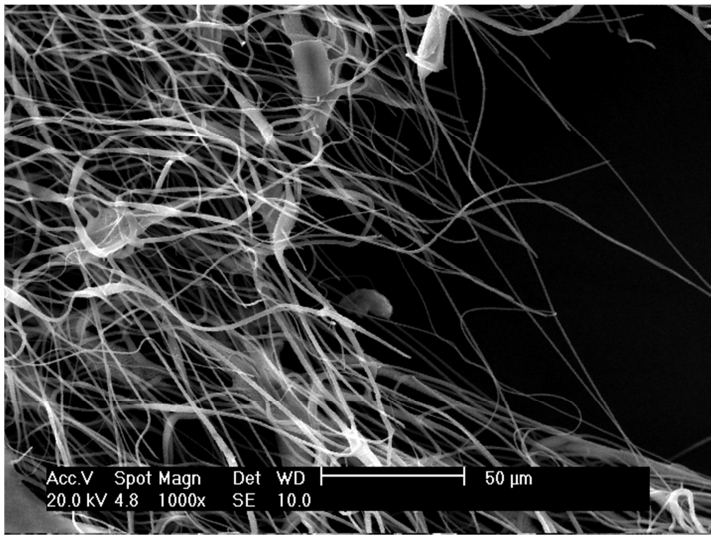


***Figure 35 –*** *SEM image of a test specimen after tensile test.*

### 4.2.3. Tear resistance

ASTM D1938 was used as a reference for the determination of the load necessary to propagate a previously started single tear in a electrospun scaffold of PLLA:PLCL. As for the tensile testing, adaptations were made to adequate the parameters for the specific structure in question (*Figure 36*).

***Figure 36 –*** *Test specimen after tear propagation.*

The resulting graphics were as in *Figure 37*; according to the standard characteristic of low extensible films.

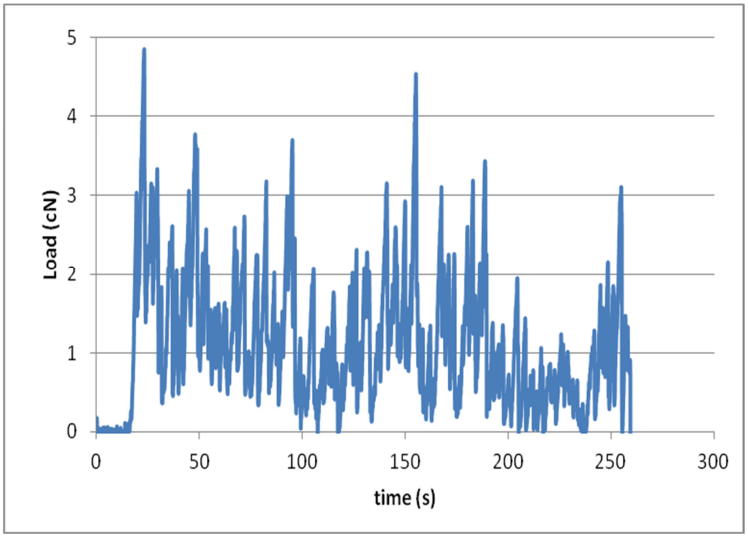


***Figure 37 –*** *Example of a load (cN) versus time (s) curve obtained for tear resistance.*

The maximum load supported ($F_{max}$) is reported in *Table 11*, and its average is 4.79cN, much lower value compared to supported stress. It is noted that dissimilar thickness of samples can invalidate the comparison of data, and so all specimens had similar thickness.

***Table 11 –*** *Results for tear propagation in a PLLA:PLCL nanofiber scaffold.*

| $F_{max}$ (cN) |
|---|
| 4.84 |
| 4.10 |
| 6.93 |
| 3.31 |
| 4.78 |
| 4.79±1.35 |

## *4.3. Cell culture*

### 4.3.1. Cell adhesion and proliferation

Through the observation of the seeded scaffolds on laser scanning microscopy CLSM it is possible to distinguish cellular distribution and penetration within the scaffold.

For this purpose, scaffolds with similar thickness – to decrease variations in cellular growth due to accessibility of nutrients – were seeded with aortic valve cells and maintained in culture up to 7 days. On different times, cultivated scaffold were fixed and colored with Hoechst – a fluorescent dye that binds to DNA and so enables the visualization of the nucleus of the cells.

*Figure 38* shows images obtained for the first, second, fifth and seventh day after seeding. To the left there is a picture from the top view of the scaffold and to the right it is possible to observe the side view for the same substrate. The cellular nuclei are marked in blue.

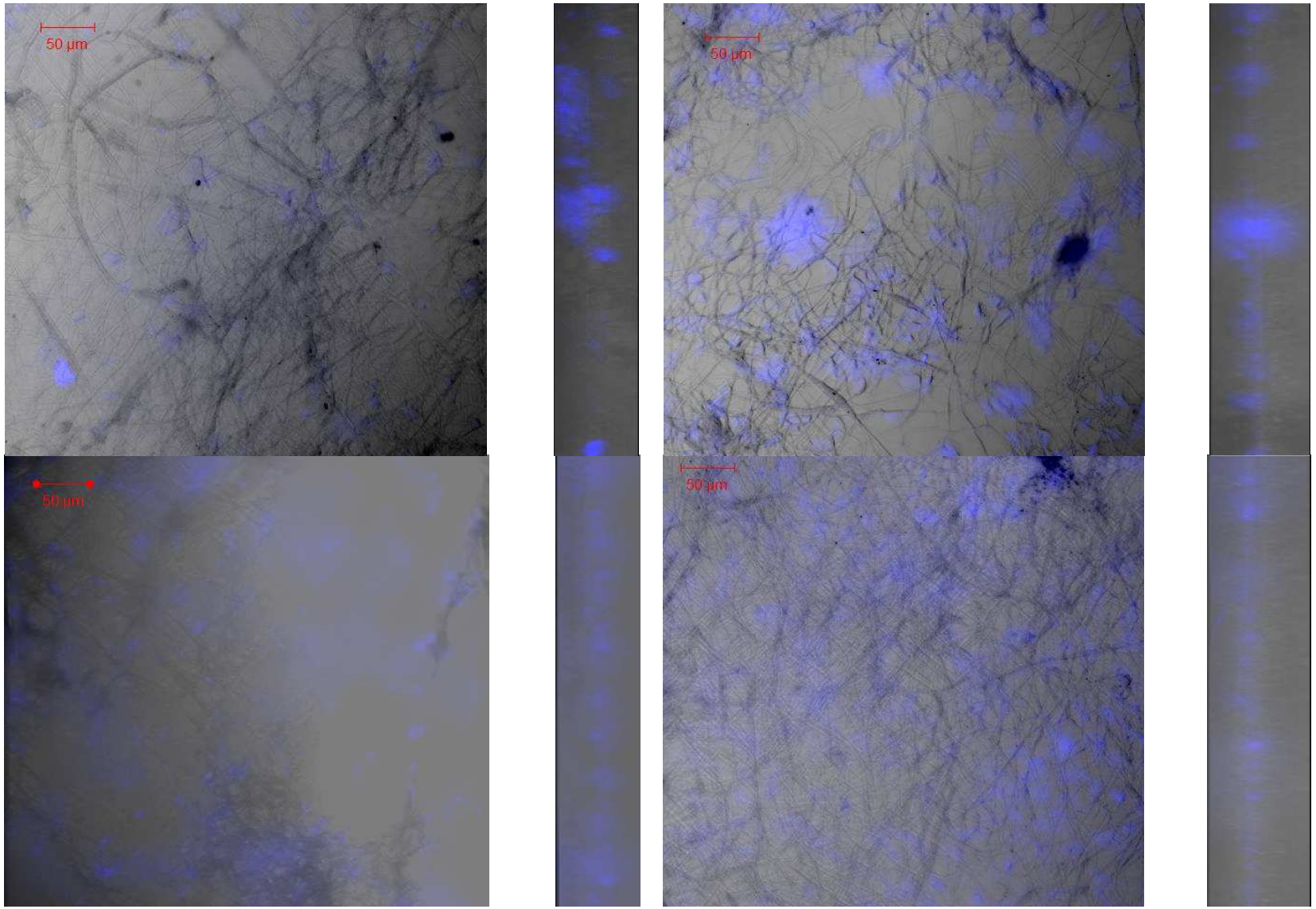


***Figure 38*** *– Scaffold a) 24h, b) 48h, c) 120h and d) 168h after seeding observed thru confocal microscope that evidences the cellular nucleus in blue.*

Even though, the cellular growth was not quantified and a discussion could be made if either the images are representative or not, it is possible to affirm the occurrence of growth and proliferation of cells in the scaffold. Other than the large difference in amount of nucleus noticed with CLSM from first to last day of cultivation, the image (*Figure 39*) acquired by optical microscopy after coloring cells with thionine (stain that colors only viable cells) supported the affirmation previously done.

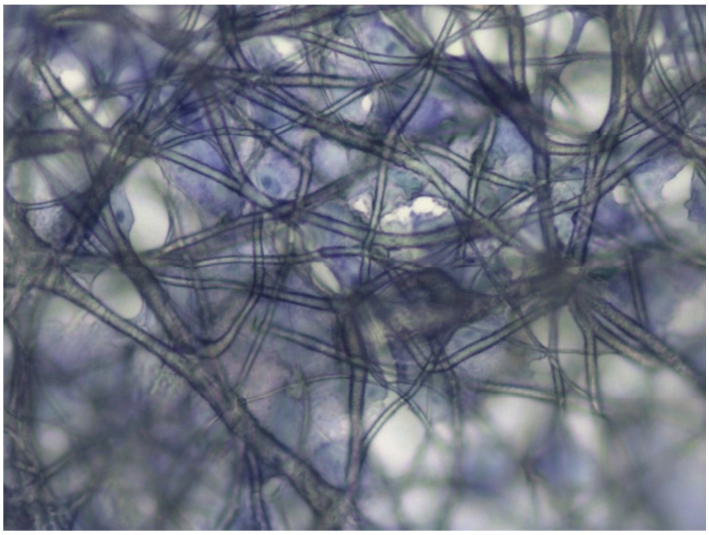

***Figure 39 –*** *Optical microscopy for cultivated scaffold with aortic valve cells for 5 days and died with thionine (40X)*

The last image also demonstrates the presence of cells within the scaffold, and not on the surface of scaffold as could be expected. From *Figure 38* side views of substrates, cells are concentrated in their middle portion, suggesting that cells did not only attached and proliferated but also penetrated thru the scaffold.

Complementary, the cultivated scaffold was observed also on SEM, making possible to observe the cellular adhesion on the substrate (*Figure 40*). The images demonstrate a good adhesion of the cells among the scaffold, while some cells are not completely adhered to the membrane. The distribution was not uniform, as it was possible the identification of agglomerations in some areas, as well as regions without any cells.

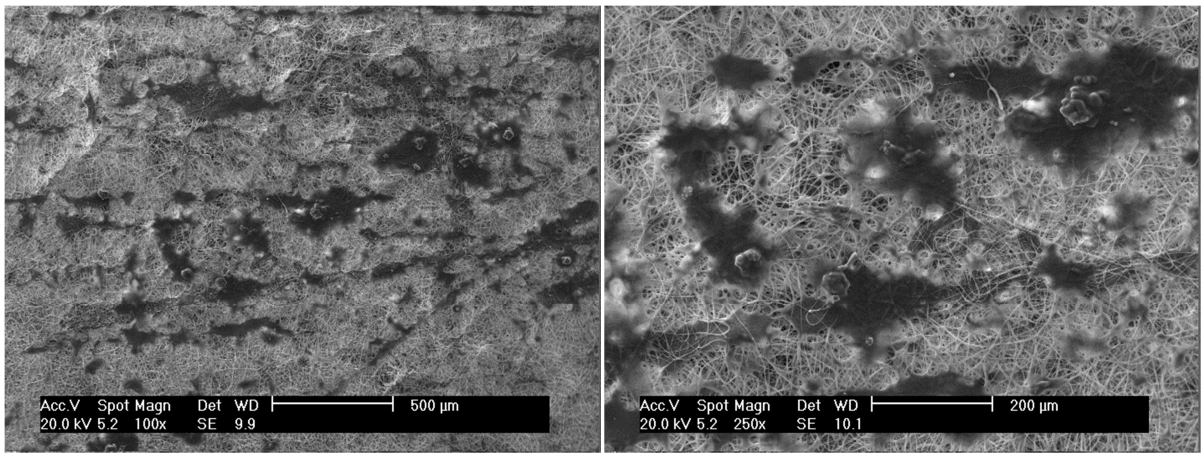


***Figure 40 –*** *SEM images for scaffolds after 4 days of cultivation.*

### 4.3.2. Cell viability

Aiming to quantify viable cells in culture, a metabolic assay was used; MTT assay provides this information quantifying the formazan crystals formed, which is directly proportional to the number of active cells in the culture (*Figure 41*). However, in the present work it would not be accurate to quantify the number of cells, since aortic valve cells is a mix of different types of cells with different active metabolism (ASTM F2739). Therefore, the method was used to quantify the growth of the cells during culture, i.e. it was used to draw a curve of cellular growth within the scaffold instead of numbering their amount (*Figure 42*).

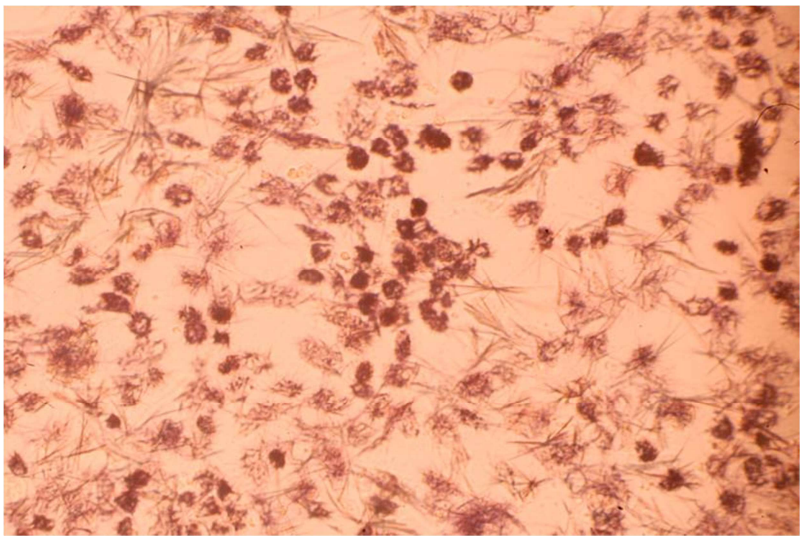

***Figure 41 –*** *Optical image of aortic valve cells after interaction with MTT; darker areas are the formed formazan (20X).*

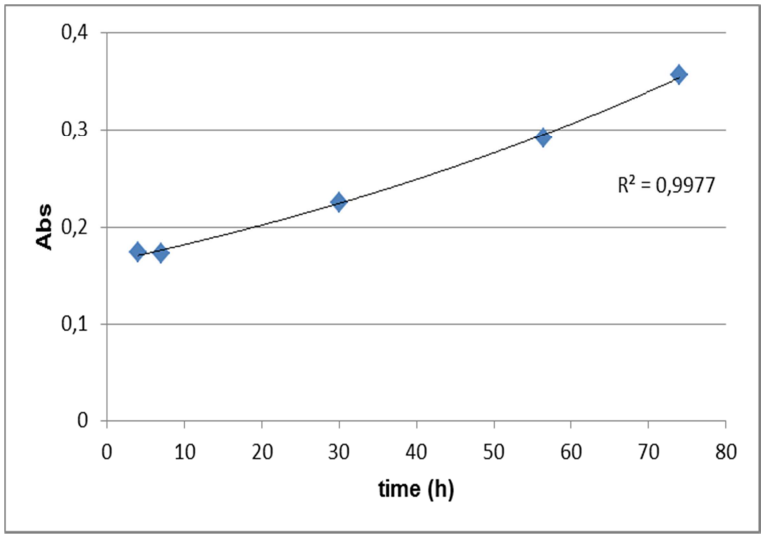


***Figure 42 –*** *Absorbance at λ=570nm versus time after scaffold seeding.*

*Figure 42* shows the increase of absorbance in an exponential curve, i.e. the increase of cellular concentration during culture. Therefore, once again the presence of viable cells is verified, but also the cellular growth is proved, demonstrating the possibility of using the scaffold for tissue engineering applications.

# 5. CONCLUSIONS

Electrospinning is a simple versatile technique for the preparation of tissue engineering scaffold, with advantages such as several polymers processed and fibers with diameters in the nanoscale allowing the substrate to have morphology similar to the ECM, high surface area and porosity. By adjusting the parameters, defect free nanofibers mats can be obtained. In the case of PLCL in concentrations up to 20%, it was not possible to produce a uniform scaffold, and so the copolymer was blended to PLLA in order to increase the viscosity of the solution, and allow the process to occur. In this sense, studies of rheology would be of great advantage for the general process, facilitating the definition of minimum concentration needed for the specific polymer.

Again adjusting the parameters, PLLA:PLCL (50:50) blend was successfully electrospun at 5% in chloroform and process parameters were voltage of 17KV, 7cm as the distance between needle and collector and flow rate of 1.236mL/h. During the process of determining the variables, it was possible to verify the influence of some of the parameters of the electrospinning process, such as concentration of the polymer solution, flow rate and applied voltage. However, the magnitude of the diameter of the electrospun fibers was not ideal, and so further improvements should be done in order to achieve the nanoscale, among them is use a smaller needle diameter, decrease concentration and increase the voltage.

The mechanical characterization of the final scaffold have shown a tensile strength of up to 1.8 MPa and elongation at break up to 9 %, while the tear resistance proved to be much smaller; the supported load was in the range of 5cN, demonstrating the fragility of this substrate to tear.

On the other hand, the seeding of the scaffolds showed growth and presence of viable cells after 7 days of culture confirming the scaffolds biocompatibility, since both polymers are well known as biocompatible, and so demonstrating the possibility of its use for tissue engineering applications. Further studies should be done to better certificate the presence and location of cells, as shouldn’t be expected cells to be penetrating the scaffold as observed in CLSM.

Moreover, future research should be done to determine the degradation rate of the final scaffold and verify the maintenance of mechanical properties for the desired application.

## REFERENCES


1. **Williams, D. F.** On the mechanisms of biocompatibility. *Biomaterials.* 2008, Vol. 29, pp. 2941-2953.
2. **Tormala, P., Pohjonen, T. and Rokkanen, P.** Ultrahigh-strength self-reinforced polylactide composites and theirs surgical applications. *Macromolecular Symposia.* 1997, Vol. 123, pp. 123-131.
3. **Middleton, J. C. and Tripton, A. J.** Synthetic biodegradable polymers as orthopedic devices. *Biomaterials.* 2000, Vol. 21, pp. 2335-2346.
4. **Marquet, V. and Jerome, R.** Design of macroporous biodegradable polymer scaffolds for cell transplantation. *Materials Science Forum.* 1997, Vol. 250, pp. 15-42.
5. **Liu, X. and Ma, P. X.** Polymeric Scaffolds for Bone Tissue Engineering. *Annals of Biomedical Engineering.* March 2004, Vol. 32, pp. 477-486.
6. **Rosso, F., et al.** Smart Materials as Scaffolds for Tissue Engineering. *Journal of Cellular Physiology.* 2005, Vol. 203, pp. 465-470.
7. **Li, W.-J. and Tuan, R. S.** Fabrication and Application of Nanofibrous Scaffolds in Tissue Engineering. *Current Protocols in Cell Biology.* 2006. In [28].
8. **Tanzi, M. C.** Fondamenti di Bioingegneria Chimica: non solo biomateriali. Pitagora Editrice Bologna. 2006.
9. **Kumar, N., Ravikumar, M. N. V. and Domb, A. J.** Biodegradable block copolymers. *Advanced Drug Delivery Reviews.* 2001, Vol. 53, pp. 23-44.
10. **Chen, F., Lee, C. N. and Teoh, S. H.** Nanofibrous modification on ultra-thin poly(e-caprolactone) membrane via electrospinning. *Materials Science and Engineering.* 2007, Vol. 27, pp. 325-332.

11. **Castro, M. L.** Copolimeros estatisticos biodegradaveis de e-caprolactona e L,L-dilactideo - sintese, caracterizaçao e propriedades. *Tese de Doutorado.* Sao Paulo: s.n., 2006.

12. **Mo, X. M., et al.** Electrospun P(LLA-CL) nanofiber: a biomimetic extracellular matrix for smooth muscle cell and endothelial cell proliferation. *Biomaterials.* 2004, Vol. 25, pp. 1883-1890.

13. **Langer, R. and Vacanti, J. P.** Tissue Engineering. *Science.* May 14, 1993, Vol. 260, pp. 920-926.

14. **Pham, Q. P., Sharma, U. and Mikos, A. G.** Electrospinning of Polymeric Nanofibers for Tissue Engineering Applications: A Review. *Tissue Engineering.* 2006, Vol. 12, pp. 1197-1211.

15. **Flemming, R. G., et al.** Effects of synthetic micro- and nano-structured surfaces on cell behavior. *Biomaterials.* 1999, Vol. 20, pp. 573-588.

16. **Chen, M., et al.** Role of fiber diameter in Adhesion and porliferation of NIH 3T3 fibroblast on electrospun polycaprolactone scaffolds. *Tissue Engineering.* 2007, Vol. 13, pp. 579-587.

17. **Mikos, A. G. and Temenoff, J. S.** Formation of highly porous biodegradable scaffolds for tissue engineering. *EJB Electronic Journal of Biotechnology.* 2000, Vol. 3, pp. 1-6.

18. **Reneker, D. H., et al.** Bending instability of electrically charged liquid jets of polymer solutions in electrospinning. *Journal of Applied Physics.* May 1, 2000, Vol. 87, pp. 4531-4547.

19. **Huang, Z.-M., et al.** A review on polymer nanofibers by electrospinning and their applications in nanocomposites. *Composites science and technology.* 2003, Vol. 63, pp. 2223-2253.

20. **Taylor, G.** Desintegration of water drops in an electric field. July 28, 1964, Vol. 280, pp. 383-397.

21. **Teo, W.-E. and Ramakrishna, S.** A review on electrospinning design and nanofibre assemblies. *Nanotechnology.* 2006, Vol. 17, pp. 89-106.

22. **Deitzel, J. M., et al.** The effect of processing variables on the morphology of electrospun nanofibers and textiles. *Polymer.* 2001, Vol. 42, pp. 261-272.

23. **Reneker, D. H. and Chun, I.** Nanometre diameter fibres of polymer, produced by electrospinning. *Nanotechnology.* 1996, Vol. 7, pp. 216–223.

24. **Shin, Y. M., et al.** Electrospinning: A whipping fluid jet generates submicron polymer fibers. *Applied Physics Letters.* February 19, 2001, Vol. 78, pp. 1-3.

25. **Liu, H. and Hsieh, Y.-L.** Ultrafine Fibrous Cellulose Membranes from Electrospinning of Cellulose Acetate. *PROCURAR.* 2002, pp. 2119-2129.

26. **Wannatong, L., Sirivat, A. and Supaphol, P.** Effects of solvents on electrospun polymeric fibers: preliminary study on polystyrene. *Polymer International.* 2004, Vol. 53, pp. 1851-1859.

27. **Fong, H., Chun, I. and Reneker, D. H.** Beaded nanofibers formed during electrospinning. *Polymer.* 1999, Vol. 40, pp. 4585-4592.

28. **Ramakrishna, S., et al.** Science and engineering of polymer nanofibers. [ed.] K. E. Geckeler and E. Rosenberg. *Functional Nanomaterials.* s.l. : ASP American Scientific Publishers E., 2006, 7, pp. 113-151.

29. **Baker, Simon C., et al.** Characterisation of electrospun polystyrene scaffolds for three-dimensional in vitro biological studies. *Biomaterials.* 2006, Vol. 27, pp. 3136–3146.

30. **Doshi, J. and Reneker, D. H.** Electrospinning process and applications of electrospun fibers. *Journal of Electrostatics.* 1995, Vol. 35, pp. 151-160.

31. **Zong, X., et al.** Structure and process relationship of electrospun bioabsorbable nanofiber membranes. *Polymer.* 2002, Vol. 43, pp. 4403-4412.

32. **Chung, S., et al.** Nanofibrous scaffolds electrospun from elastomeric biodegradable poly(L-lactide-co-ε-caprolactone) copolymer. *Biomedical Materials.* February 4, 2009, Vol. 4, pp. 1-10.

33. **Boland, E. D., et al.** Tailoring tissue engineering scaffolds using electrostatic processing technicques: a study of poly(glycolic acid) electrospinning. *Journal Macromolecular Science.* 2001, Vol. 12, pp. 1231-1243.

34. **Chen, F., et al.** Electrospun chitosan-P(LLA-CL) nanofibers for biomimetic extracellular matrix. *Journal of Biomaterial Scienc Polymer Edn.* 2008, Vol. 19, pp. 677-691.

35. **Casper, C. L., et al.** Controlling Surface Morphology of Electrospun Polystyrene Fibers: Effect of Humidity and Molecular Weight in the Electrospinning Process. *Macromolecules.* 2004, Vol. 37, pp. 573-578.

36. **Edwards, M. D., et al.** Deveopment of orientation during electrospinning of fibers of poly(e-caprolactone). *European Polymer Journal.* March 22, 2010, Vol. 46, pp. 1175-1183.

37. **Kwon, O. H., et al.** Electrospun nanofibers for biomedical applications. [ed.] K. Ariga and H. S. Nalwa. *Bottom-up nanofabrication supramolecules, self-assemlies and organized films.* s.l. : ASP American Scientific Publishers E., 2009, Vol. 6, 1, pp. 1-16.

38. **Xu, C., et al.** Electrospining nanofiber fabrication as synthetic extracellular matrix and its potential for vascular tissue engineering. *Tissue Engineering.* 2004, Vol. 10, pp. 1160-1168.

39. **Li, X., et al.** Encapsulation of proteins in poly(l-lactide-co-caprolactone) fibers by emulsion electrospinning. *Colloids and Surfaces B: Biointerfaces.* 2010, Vol. 75, pp. 418–424.

40. **Ramos, S. LF, et al.** *Redes de policaprolactona (PCL) obtidas por "electrospinning": principais propriedades e aplicaçoes como biomaterial.* s.l. : COLAOB - The 6th Latin American Congress of Artificial Organs and Biomaterials, tesi.

41. **Lee, K. H. et al.** The change of bead morphology formed on electrospun polystyrene fibers. *Polymer.* 2003, Vol. 44, pp. 4029-4034.

42. **Young, Y., et al.** In vitro degradation behavior of electrospun polyglucolide, polylactice and poly(lactide-co-glycolide). *Journal of Applied Polymer Science*. 2004, Vol. 95, pp. 193-200.

43. **Teo, W.-E., He, W. and Ramakrishna, S.** Electrospun scaffold tailored for tissue-specific extracellular matrix. *Biotechnology Journal.* 2006, Vol. 1, pp. 918-929.

44. **Castro, M. L. de and Wang, S. H.** Statistical copolymers of l.l-lactide and e-caprolactone. *Polymer Bulletin*. 2003, Vol. 51, pp. 151-158.

45. **Mothé, C., Drumond, W. S. and Wang, S. H.** Phase behavior of biodegradable amphiphilic poly(l,l-lactide)-b-poly(ethylene glycol)-b-poly(l,l-lactide). *Thermochimica Acta*. 2006, Vol. 445, pp. 61-66.